P. O. TJØM AND B. ELBEK

A STUDY OF ENERGY LEVELS IN ODD-MASS GADOLINIUM NUCLEI BY MEANS OF (*d*,*p*) AND (*d*,*t*) REACTIONS

Det Kongelige Danske Videnskabernes Selskab
Matematisk-fysiske Meddelelser **36**, 8

Kommissionær: Munksgaard
København 1967

CONTENTS

		Page
1.	Introduction	3
2.	Theoretical Cross Sections	4
3.	Experimental Procedures	7
4.	Results and Discussion	8
4.1.	Q-Values	8
4.2.	General Features of the Spectra	19
4.3.	Detailed Interpretation of the Spectra	22
	4.3.1. The $3/2-[521]$ Orbital	23
	4.3.2. The $5/2+[642]$ and the $3/2+[651]$ Orbitals	25
	4.3.3. The $1/2+[660]$ Orbital	28
	4.3.4. The $11/2-[505]$ Orbital	29
	4.3.5. The $3/2+[402]$ and the $1/2+[400]$ Orbitals	31
	4.3.6. The $3/2-[532]$ Orbital	34
	4.3.7. The $1/2-[530]$ Orbital	36
	4.3.8. The $7/2+[404]$ Orbital	39
	4.3.9. The $5/2-[523]$ Orbital	40
	4.3.10. The $1/2-[521]$ Orbital	42
	4.3.11. The $7/2+[633]$ Orbital	43
	4.3.12. The $5/2-[512]$ Orbital	44
	4.3.13. The $1/2-[510]$ Orbital	45
	4.3.14. The $1/2+[651]$ Orbital	46
	4.3.15. Other Levels in the Deformed Nuclei	46
	4.3.16. Levels in ^{153}Gd and ^{151}Gd	48
5.	Comparison of Intensities with Predicted Values	48
6.	Conclusions	52
	References	54

Synopsis

The energy levels of ^{151}Gd, ^{153}Gd, ^{155}Gd, ^{157}Gd, ^{159}Gd, and ^{161}Gd have been investigated by means of (d,p) and (d,t) reactions on the stable even gadolinium isotopes. The deuteron energy was 12.1 MeV and the charged reaction products were analyzed in a magnetic spectrograph at 60°, 90°, and 125°. Application of theoretical and semi-empirical rules for the cross sections allowed the identification of states belonging to 16 different Nilsson orbitals, most of them in several nuclei. In the lighter gadolinium nuclei, the onset of deformation gives rise to complicated level structures which only in part can be explained by the Nilsson model. The spectra of these nuclei also show several effects which can be ascribed to the crossing of levels with the same spin and parity, but belonging to different oscillator shells. The experimental level scheme based on the observation of the $7/2+[404]$ and $1/2+[651]$ Nilsson orbitals in ^{159}Gd is compressed by approximately a factor of two compared to the theoretical level scheme.

PRINTED IN DENMARK
BIANCO LUNOS BOGTRYKKERI A/S

Introduction

In an earlier investigation[1], the energy levels of the odd isotopes of ytterbium were studied by means of (d,p) and (d,t) reactions induced by 12 MeV deuterons. The main results of this investigation were the systematic localization of a number of Nilsson states as a function of the neutron number and the experimental proof that the cross sections for population of these states by single-neutron transfer reactions to a surprising accuracy were obtained from the Nilsson[2] wave functions, the distorted wave Born approximation (DWBA) formalism[3], and the pairing theory. It was therefore indicated that the low lying levels in ytterbium represent relatively pure single-particle motions. However, in a few cases, significant deviations from the simple scheme outlined above were observed. Some of the deviations could be related to the coupling of the single particle to the collective gamma vibration, and a microscopic treatment[4] of this coupling gave qualitative agreement with the experimental results. At higher excitation energies, the presence of other couplings became evident, but no detailed analysis of the relevant experimental material was attempted.

This work extends the earlier investigation into the odd Gd nuclei in the beginning of the region of deformed rare earth nuclei.

For several reasons, the situation in the Gd nuclei is expected to be more complex than it was the case for the Yb nuclei. In the beginning of the deformed region, the deformation is rapidly changing with the neutron number. In fact, the lightest nuclei investigated here, ^{151}Gd and ^{153}Gd, cannot be assumed to possess any stable deformation. Furthermore, the even Gd nuclei show low lying, strongly collective excitations[5] of quadrupole and octupole type, in contrast to the even Yb nuclei where these excitations are high lying and weak[6]. Finally, the single-particle spectrum in the Gd nuclei contains several near lying states with the same parity and a K-quantum number differing by zero or one unit. Such states are probably strongly mixed.

On the other hand, the low-energy spectrum of the Gd nuclei is expected to show the presence of single-particle levels from the $N = 4$ oscillator shell.

These states have large components of the $s_{1/2}$, $d_{3/2}$ or $g_{7/2}$ shell-model orbitals and are predicted to have large cross sections for the neutron transfer processes. Especially large (d,t) cross sections can be expected in the Gd nuclei, as the $N = 4$ states there will occur as hole excitations.

Some assistance in the analysis of the (d,t) spectra was provided from the measurement of the triton angular distributions for the ^{160}Gd$(d,t)^{159}$Gd reaction[7]. The relatively simple spectrum of the ^{159}Gd nucleus made it possible to obtain angular distributions for triton groups where the orbital angular momentum, l, of the neutron picked up had values of 0, 1, 2, 3, 4, 5 or 6. These distributions could then be used as references for the analysis of more complicated cases in other nuclei.

Finally, the (d,d') spectra for the odd nuclei ^{155}Gd and ^{157}Gd have been useful in the analysis of levels with collective admixtures. A detailed account of the (d,d') experiments will be published separately[8].

2. Theoretical Cross Sections

For reference, we here list a few formulae which have been used in the comparison of the experimental cross sections to those obtained from theory.

The theory of stripping and pick-up for a deformed target nucleus has been given by SATCHLER[9]. When the target nucleus is even and has spin 0, the cross section for stripping leading to a rotational level with spin $I_f = j$ can be written

$$\frac{d\sigma}{d\Omega} = 2C_{j,l}^2 \varphi_l(\theta) U^2, \tag{1}$$

where the factor U^2 approximately takes into account the effect of the partial filling of the neutron orbital in the target nucleus. The $C_{j,l}$ is the expansion coefficient of the Nilsson wave function on the spherical wave functions. These coefficients have been tabulated by several authors[10, 11, 12]. The angular function $\varphi_l(\theta)$ is obtained from the DWBA calculation for the transfer of a neutron with orbital angular momentum l. For the present work, the $\varphi_l(\theta)$ functions were obtained from a GIER ALGOL computer code[13] similar to the well-known code SALLY[3]. The optical model parameters for the deuteron, proton and triton potentials used in the calculations are listed in table 1. The deuteron and proton potentials are essentially the same as those used for the anaylsis of the Yb data[1], whereas the triton potentials are those found from the analysis of the ^{160}Gd(d,t) angular distributions[7].

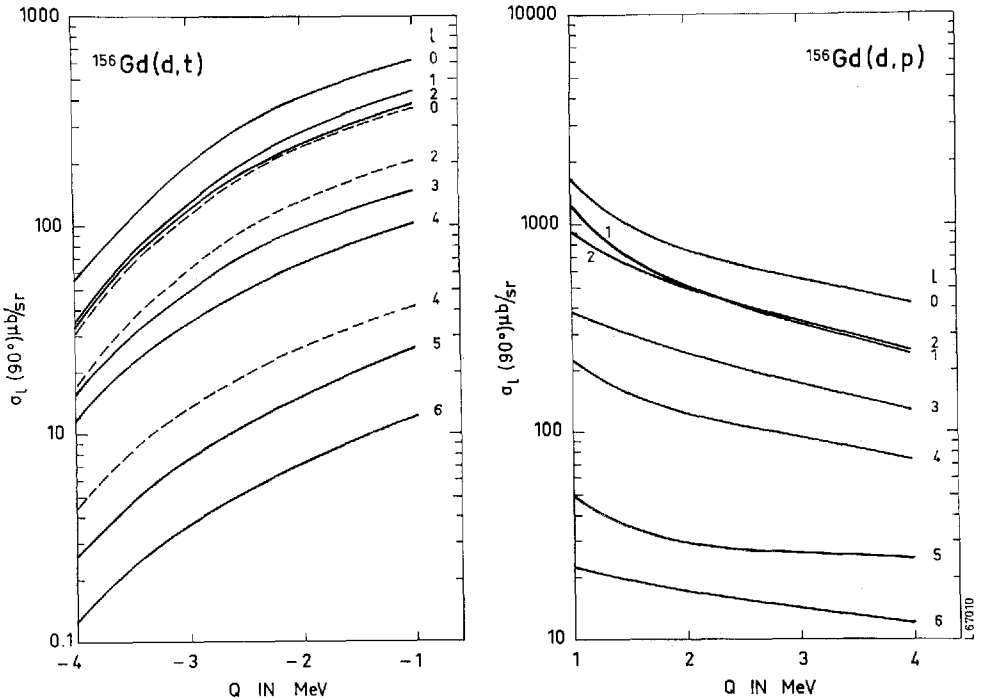

Fig. 1. Q-dependence of the single-particle cross section $\sigma_l(\theta)$. The odd l-values correspond to the $N = 5$ oscillator shell. For the even l-values the curves for $N = 6$ are drawn full, those for $N = 4$ dotted.

The $\varphi_l(\theta)$ function in eq. (1) differs from that obtained from the DWBA calculation by a normalization factor N. If $\sigma_l(\theta)$ is the result of the DWBA calculation, we use the normalization $\varphi_l(\theta) = 1.5\,\sigma_l(\theta)$ for the (d,p) reactions, which is in agreement with common practice. For the (d,t) reaction we use the empirical relationship $\varphi_l(\theta) = 3.0\,\sigma_l(\theta)$.

The $\varphi_l(\theta)$ functions depend on the Q-value of the transfer reaction. For a comparison of the data obtained for the different nuclei it was found useful to reduce all the experimental cross sections to a standard Q-value by means of the theoretical Q-dependence which is shown in fig. 1. The (d,p) cross sections were reduced to $Q = 3.0$ MeV, whereas the (d,t) cross sections were reduced to $Q = -2.0$ MeV. For cases in which the l-values were not known, the Q-dependence for $l = 2$ was used. When the data were compared for levels with definite assignments, calculations for the proper values of l and the oscillator quantum number N were used.

Equation (1) applies only to pure Nilsson states. The experimental

material presented here contains several cases where strong mixing of the wave functions for two or more levels is indicated. If the wave function for a level contains admixtures with amplitudes a_i of other levels, then the stripping cross section for the n'th level is taken to be

$$\frac{d\sigma_n(\theta)}{d\omega} = 2(\sum_i C_{j,l}^{(i)} U_i a_{in})^2 \varphi_l(\theta), \tag{2}$$

where the $C_{j,l}^{(i)}$ refers to the expansion coefficient for the i'th level and U_i to the corresponding pairing factor. The pick-up cross section is obtained by replacing U_i by the pairing factor V_i.

An especially important coupling is the Coriolis coupling between rotational bands differing by one unit in K-quantum number. If we limit ourselves to two bands, K and $K+1$, then the Coriolis matrix[14] element is

$$A_K = -\frac{\hbar^2}{2\Im} \langle K|j_-|K+1\rangle (U_K U_{K+1} + V_K V_{K+1}), \tag{3}$$

where $\Im$ is the nuclear moment of inertia and j_- denotes the usual total angular momentum lowering operator. The last factor in (3) takes into account the pairing[15]. The matrix elements j_- can be expressed in terms of the $C_{j,l}$ coefficients

$$\langle K|j_-|K+1\rangle = \sum_{j,l} C_{j,l}^{(K)} C_{j,l}^{(K+1)} \sqrt{(j-K)(j+K+1)}. \tag{4}$$

The admixed amplitudes can be calculated according to KERMAN[14]. However, in order to avoid ambiguities in the relative signs of the expansion coefficients, we here give a consistent set of formulae for the case $E_{K+1} - E_K > 0$, where E refers to the unperturbed level energy. The perturbed wave functions, u, of level 1 or 2 can then be expressed by

$$u^{(1,2)} = a_K^{(1,2)} u_K + a_{K+1}^{(1,2)} u_{K+1} \tag{5}$$

and the perturbed energies as

$$E^{(1,2)} = \tfrac{1}{2}(E_{K+1} + E_K) \pm \tfrac{1}{2}\sqrt{(E_{K+1} - E_K)^2 + 4A_K^2(j-K)(j+K+1)}. \tag{6}$$

The amplitues, a, are determined by

$$a_K^{(1,2)} = \left\{1 + \left[\pm R + \sqrt{1+R^2}\right]^2\right\}^{-\frac{1}{2}}; \quad a_K^2 + a_{K+1}^2 = 1, \tag{7}$$

where

$$R = \frac{E_{K+1} - E_K}{2A_K\sqrt{(j-K)(j+K+1)}}. \tag{8}$$

The signs are determined by the rules

$$\left.\begin{aligned} &\text{if } A_K < 0, \text{ then } a_K^{(1)}/a_{K+1}^{(1)} < 0 \text{ and } a_K^{(2)}/a_{K+1}^{(2)} > 0 \\ &\text{if } A_K > 0, \text{ then } a_K^{(1)}/a_{K+1}^{(1)} > 0 \text{ and } a_K^{(2)}/a_{K+1}^{(2)} < 0. \end{aligned}\right\} \tag{9}$$

If $E_{K+1} - E_K < 0$, a_K and a_{K+1} are interchanged in equation (7) and the signs determined by (9) are reversed.

3. Experimental Procedures

The experimental methods closely follow those of ref.[1]. A 12.1 MeV deuteron beam was obtained from the Niels Bohr Institute tandem accelerator. The reaction products from a thin target were analyzed in a broad-range magnetic spectrograph and recorded on photographic plates which were scanned manually to obtain the particle intensity as a function of the distance along the plate.

The targets for this investigation were prepared by the University of Aarhus isotope separator group by direct deposition of the separated isotopes on carbon foils, about 40 μg/cm^2 thick. The exposures in the magnetic spectrograph, which here are analyzed for proton tracks and triton tracks, are identical to those analyzed for deuteron tracks in ref.[5].

A few improvements in the experimental techniques described in ref.[1] have been introduced for the present series of measurements. In most cases, three angles, 60°, 90° and 125°, were measured immediately after each other. For the 60° and 90° exposures, the target was left in the same position (transmission geometry) whereas the target was turned for the 125° exposure (reflection geometry). The use of the same target and identical beam conditions for all angles greatly improved the accuracy of the relative cross section determinations and has made it possible to draw some conclusions about angular momenta on the basis of intensity changes with angle.

The magnetic spectrograph was carefully recalibrated over the full energy range. The role of partial saturation in the iron was evaluated, but the effects were found to be negligible for the field strengths used in the present work ($B_{\max} \sim 10.000$ Gauss).

The intensity of the beam obtainable from the tandem accelerator has gradually been improved, which made it possible to use smaller beam de-

TABLE 1. Optical model parameters for deuterons, tritons, and protons.

	V MeV	W MeV	r_0 fm	a fm	r_0' fm	a' fm	r_c fm
(d,p) deuteron parameters	86	12	1.15	0.87	1.37	0.70	1.25
proton parameters	54	15	1.25	0.65	1.25	0.47	1.25
(d,t) deuteron parameters	86	12	1.15	0.87	1.37	0.70	1.25
triton parameters	154	12	1.10	0.75	1.40	0.65	1.25

fining apertures. As a rule, beams of 0.7 μA through two 0.55×3 mm^2 apertures were used. The resulting resolution (FWHM) was approximately 9 keV for the (d,t) spectra, whereas the (d,p) spectra, which mostly were recorded at the low dispersion part of the photographic plate, rarely showed resolutions better than about 13 keV.

Somewhat improved excitation energy determinations were obtained by the use of the center-of-gravity of a peak for position definition instead of the usual 1/3 intensity point on the high energy side of the peak. The accuracy of the Q-values is estimated to be ± 10 keV, whereas the accuracy of the excitation energies is ± 3 keV below 1 MeV of excitation, and otherwise ± 5 keV.

4. Results and Discussion

Gadolinium has five stable even isotopes which all were used as targets in the present investigation. Thus, the energy levels in the odd nuclei from ^{151}Gd to ^{161}Gd could be investigated by at least one of the reactions (d,p) and (d,t).

A spectrum for each of the ten different reactions is shown in figures 5–14. The level energies obtained as the average of the determinations at three angles are listed in tables 2–7, which contain also the measured differential cross sections and the suggested Nilsson assignments for some of the levels. The basis for these assignments will be discussed in detail in the following sections.

4.1. Q-Values

The localization of the ground state poses no problem in the final nuclei from ^{161}Gd to ^{155}Gd where the low energy spectrum is well known. For ^{153}Gd, it is possible uniquely to relate the spacings of levels observed by the transfer reactions to spacings of levels known from decay studies. Thereby

TABLE 2. Levels populated in ^{151}Gd.

Energy average (d,t) keV	Assignment	$d\sigma/d\Omega$ (d,t) $\mu b/sr$		
		60°	90°	125°
0	$(f7/2)$	387	358	
108		7	6	
375		10	25	
394		99	119	
424		23	21	
584		72	66	26
616		26	21	13
666		48	54	34
697		4	6	5
707		1	2	5
806		14	11	3
835		41	28	16
847		7	7	8
882		1	2	
907		3	2	
977	$(d3/2)$	138	190	129
1047	$(s1/2)$	137	178	124
1083		12	5	3
1156		21	14	15
1190		22	30	15
1204		14	29	25
1357			19	13

the ground state is also established. A similar correspondence can be obtained for ^{151}Gd, but for fewer energy levels. The Q-values for the ground states are collected in table 8 which also lists the neutron separation energies derived from the data by means of the expressions

$$\left.\begin{aligned} S_n(A) &= 6.258\,\text{MeV} - Q_{d,t} \text{ for } A \rightarrow A-1 \\ S_n(A) &= 2.225\,\text{MeV} + Q_{d,p} \text{ for } A-1 \rightarrow A. \end{aligned}\right\} \quad (10)$$

Table 8 includes also the data for the odd target nuclei of Gd, which will be discussed separately[16]. It should be noted that the independent determinations of the separation energies by (d,p) and (d,t) reactions are in good agreement with each other, which gives some confidence in the accuracy of the absolute values of Q. Also the agreement with the most recent mass spectroscopic two-neutron separation energies[17] is satisfactory.

TABLE 3. Levels populated in ^{153}Gd.

Energy average		Assignment	$d\sigma/d\Omega(d,p)$ $\mu b/sr$			$d\sigma/d\Omega(d,t)$ $\mu b/sr$		
(d,p) keV	(d,t) keV		60°	90°	125°	60°	90°	125°
0	0		94	39	12	100	94	41
43	43		~ 6	~ 1	~ 1	~ 1		~ 2
93	94		630	405	171	178	197	118
110	110		60	36	22	42	50	27
138	140	11/2 11/2 − [505]?	52	53	40	14	28	26
	172					21	49	41
182	183		23	16	2	14	18	13
217	213	3/2 3/2 + [402]	110	72	55	326	385	273
	251					10	13	13
	304					9	16	12
315	315		31	15	6	22	9	7
328	328	1/2 1/2 + [400]	25	12	6	346	390	260
363	363	3/2 1/2 − [530]	445	232	97	155	144	24
	394					2	8	25
435	431		369	148	65	25	15	18
	441					7	26	21
	483						10	11
507	504		189	78	40	38	50	44
530	533		136	64	29	4	6	
548	546		65	46	22	2	4	
575			10	6	4			
	580					10	17	19
606	606		24	15	10	2	3	
634			14	18	11			
648	646		29	27	7	4	3	
678			37	34	11			
721			71	41	20			
736			11	4				
772	773		147	103	59	11	16	14
856		1/2 1/2 − [521]	427	189	65			
876			27	25	19			
	883					6	13	9
889			28	26	17			
905			52	38	21			
943		3/2 1/2 − [521]	55	30	14			
960		5/2 1/2 − [521]	175	63	25			
	983					3	4	
994			89	39	21			

(continued)

TABLE 3 (continued).

Energy average		Assignment	$d\sigma/d\Omega(d,p)$ $\mu b/sr$			$d\sigma/d\Omega(d,t)$ $\mu b/sr$		
(d,p) keV	(d,t) keV		60°	90°	125°	60°	90°	125°
1034			19	10	4			
1052			64	35	15			
1081			9	5				
1099			22	16	7			
1115			8	6	3			
	1116					12		23
1143			24	21	9			
1155	1151	7/2 1/2 − [521]	82	39	25	15		36
1171			193	94	37			
1194		9/2 1/2 − [521]	12	6	3			
1235			27	14	10			
1251			27	9	5			
	~ 1287	7/2 7/2 + [404]				~ 49		
1296			60	23	15			
1339			19	7	8			
1361			139	62	32			
1384			76	35	15			
1400			67	35	15			
1421			65	36	18			
1448			58	25	8			
1482			49	31	20			
1496			37	20	12			
1509			43	25	32			
1533			42	25	13			
1548			71	48	26			
1564			39	15	7			
1584			51	37	15			
1597			28	19	9			
1615			47	26	14			
1631			13	10	8			
1655			51	31	13			
1669			22	13	5			
1686			34	13	10			
1701			18	13	8			
1720			65	30	13			
1738			47	26	12			
1755			69	36	15			
1772			34	25	9			

TABLE 4. Levels populated in ^{155}Gd.

Energy average		Assignment	$d\sigma/d\Omega(d,p)$ $\mu b/sr$			$d\sigma/d\Omega(d,t)$ $\mu b/sr$		
(d,p) keV	(d,t) keV		60°	90°	125°	60°	90°	125°
0	0	3/2 3/2 – [521]	118	43	33	78	58	22
~ 60	~ 60	5/2 3/2 – [521]	~ 4	~ 3		~ 2	~ 1	
~ 81	~ 83		~ 4	~ 3		~ 8	~ 12	~ 7
107	106		114	83	35	239	241	129
	119	11/2 11/2 – [505]				84	97	49
145	145	7/2 3/2 – [521]	227	138	64	100	92	41
213	214		59	48	37	31	56	35
247	250	9/2 3/2 – [521]	28	10	5	5	10	6
267	267	3/2 3/2 + [402]	74	59	28	340	343	210
287	282		16	9		30	32	9
321	322	5/2 5/2 – [523]	50	28	20	108	95	40
	345					2	4	8
367	367	1/2 1/2 + [400]	129	56	28	608	594	319
392	393	7/2 7/2 – [523]	117	90	42	23	49	22
422	~ 423	1/2 1/2 – [530]	20	9	8	34	~ 16	~ 16
	~ 428						~ 32	~ 25
450	451	3/2 1/2 – [530]	170	89	34	405	328	129
485		9/2 5/2 – [523]	29	25	20			
	489	5/2 1/2 – [530]				77	101	80
	556	7/2 1/2 – [530]				57	50	14
556		1/2 1/2 – [521]	401	200	95			
	594	β-vib, 3/2 3/2 – [521]				20	12	11
614		3/2 1/2 – [521]	75	36	13			
	617	9/2 1/2 – [530]				8	7	4
658	659	5/2 1/2 – [521]	81	36	23	5	4	
692			19	8	13			
	721	β-vib, 7/2 3/2 – [521]				13	24	12
751	753		31	17	3	23	25	7
784	787	7/2 1/2 – [521]	153	98	46	4	5	4
	813	β-vib, 9/2 3/2 – [521]				8	4	4
866	867	9/2 1/2 – [521]	12	11		5	4	
1005			38	21				
1025			48	41				
1082			28	7				
1110			26	21				
	1118					1	4	
1131			51	42				
1160*			13	16				

* Several unresolved peaks from 1160 keV to 1250 keV.

(*continued*)

TABLE 4 (continued).

Energy average		Assignment	$d\sigma/d\Omega(d,p)$ $\mu b/sr$			$d\sigma/d\Omega(d,t)$ $\mu b/sr$		
(d,p) keV	(d,t) keV		60°	90°	125°	60°	90°	125°
1191			14	7				
	1239					4	4	
1241			16	8				
	1267					7	2	
	1295	7/2 7/2 + [404]				67	~ 95	80
1303			60	33				
	1331					2	3	
1339			44	16				
	1357					~ 1	4	
1362			44	26				
1408			31	21				
1438			69	66				
1472			70	38				
1518			40	21				
1548			65	41				
1563			31	14				
1587			32	9				
1604			83	37				
1626			233	125				
1653			41	18				
1704			28	20				
1745			63	53				
1794			66	41				
1822			42	31				
1843			175	84				
1869			55	20				
1899			53	33				
1932			79	42				

In fig. 2 the neutron separation energies are shown as function of the mass number. The most noticeable feature is the decrease in $S_n(A)$ for the lighter nuclei. This effect is undoubtedly related to the onset of deformation.

It is also noted that the differences in S_n between even and odd nuclei are largest for the most neutron deficient nuclei. A similar trend has been observed for other series of isotopes in the rare earth region and implies an increase in the neutron pairing energies as the number of neutrons is reduced. The occurrence of strongly collective states in the neutron deficient nuclei[5] may probably be related to a corresponding increase in the energy gap.

TABLE 5. Levels populated in ^{157}Gd.

Energy average		Assignment	$d\sigma/d\Omega(d,p)$ $\mu b/sr$			$d\sigma/d\Omega(d,t)$ $\mu b/sr$	
(d,p) keV	(d,t) keV		60°	90°	125°	60°	90°
0	0	3/2 3/2 − [521]	146	55	23	205	100
	~ 53	5/2 3/2 − [521]					~ 2
~ 62	~ 63	5/2 5/2 + [642]		~ 2	~ 3	~ 1	~ 2
	~ 115	7/2 5/2 + [642]				4	3
133	132	7/2 3/2 − [521]	236	132	69	232	150
181	181	9/2 5/2 + [642]	55	25	18	75	65
228	227	9/2 3/2 − [521]	23	9	11	10	13
~ 276		11/2 5/2 + [642]	4	3	2		
315			6	3			
~ 346	~ 349	11/2 3/2 − [521]		5	8	4	9
360	361	13/2 5/2 + [642]	62	50	40	38	49
	~ 372					~ 3	~ 3
	426	11/2 11/2 − [505]				36	69
435	435	5/2 5/2 − [523]	51	28	21	25	24
478	475	3/2 3/2 + [402]	75	31	21	554	404
	513					44	46
518	523	7/2 5/2 − [523]	206	103	64	5	9
617	618	9/2 5/2 − [523]	44	20	20	5	11
665	665		18	6	5	49	37
686	684	1/2 1/2 + [400]	117	70	45	1080	844
	700	3/2 3/2 − [532]?				58	59
704		1/2 1/2 − [521]	359	128	60		
	718					85	45
745	744	3/2 1/2 − [521]	21	20	6	6	9
	751	5/2 3/2 − [532]?				6	13
	770					8	10
	792					104	66
795		5/2 1/2 − [521]	116	70	44		
812	809	3/2 1/2 − [530]	178	84	26	346	260
	813	7/2 3/2 − [532]?				190	143
834			84	38	25		
	837	5/2 1/2 − [530]				65	43
	850					8	20
	901	7/2 1/2 − [530]				22	20
903		7/2 1/2 − [521]	78	39	23		
	918	9/2 3/2 − [532]?				6	7
	962	9/2 1/2 − [530]				11	~ 12
965			78	51	36		
	981					8	6

(continued)

TABLE 5 (continued).

Energy average (d,p) keV	Energy average (d,t) keV	Assignment	dσ/dΩ(d,p) μb/sr 60°	dσ/dΩ(d,p) μb/sr 90°	dσ/dΩ(d,p) μb/sr 125°	dσ/dΩ(d,t) μb/sr 60°	dσ/dΩ(d,t) μb/sr 90°
~ 988		9/2 1/2 – [521]		~ 4			
1039			9	~ 4	3		
	~ 1060	11/2 1/2 – [530]				2	
	1093					21	
	1113					3	
1117			61	43	27		
	1141					31	22
1142			38	14	17		
	1175					3	6
1185				5	2		
	1203					~ 1	3
1206				5	5		
	1246					5	3
1289			5	3	3		
	1296					21	11
	1305					9	7
1312			37	13	7		
	1316					2	3
1331			9	7	4		
	1339					4	5
	1352					2	4
1354			14	11	7		
1391		7/2 5/2 – [512]?	114	95	54		
	1396					4	6
	1414					5	3
1437			10	2			
	1466					3	6
1472			38	19	14		
1487			52	19	15		
1519			24	5	7		
	1524					4	4
1555			11	11	7		
	1556					27	23
	1569					5	11
	1589					30	31
1593			112	50	38		
	1611					6	4
1614			22	17	14		
	1635					3	4

(continued)

TABLE 5 (continued).

Energy average		Assignment	$d\sigma/d\Omega(d,p)$ $\mu b/sr$			$d\sigma/d\Omega(d,t)$ $\mu b/sr$	
(d,p) keV	(d,t) keV		60°	90°	125°	60°	90°
1660			43	34	20		
	1670					2	4
	1720					4	6
	1731					8	7
	1738					12	19
1744			123	62	27		
1767			21	11	8		
1793			68	19	18		
1809			39	15			
	1811					9	6
	1825	7/2 7/2+[404]				56	61
1833			47	35			
1845			81	35			
1869			80	40			
1906			206	188			
1929			45	27			

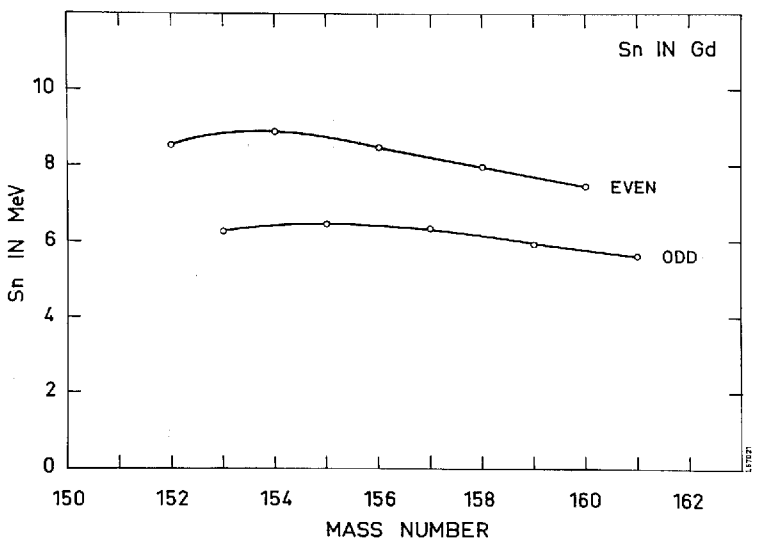

Fig. 2. Neutron separation energy as a function of the mass number.

TABLE 6. Levels populated in ^{159}Gd.

Energy average		Assignment	$d\sigma/d\Omega(d,p)$ $\mu b/sr$			$d\sigma/d\Omega(d,t)$ $\mu b/sr$		
(d,p) keV	(d,t) keV		60°	90°	125°	60°	90°	125°
0	0	3/2 3/2 − [521]	155	66	24		191	73
	~ 50	5/2 3/2 − [521]				~ 4	~ 4	~ 2
	67	5/2 5/2 + [642]				~ 3	~ 4	~ 2
122	120	7/2 3/2 − [521]	148	88	39	298	219	91
147	146	5/2 5/2 − [523]	47	22	12	42	27	10
185	184	9/2 5/2 + [642]	49	29	13	112	86	38
	211	9/2 3/2 − [521]				17	22	12
227	226	7/2 5/2 − [523]	242	136	49	140	118	45
~ 275	~ 272	11/2 5/2 + [642]	7	~ 3	~ 2	~ 2	~ 3	~ 1
330	327	11/2 3/2 − [521] 9/2 5/2 − [523]	27		17	11	25	11
373	371	13/2 5/2 + [642]	50		33	58	71	47
457	455	11/2 5/2 − [523]	22	18	13	10	18	16
507	506	1/2 1/2 − [521]	525	199	81	146	80	20
559	557	3/2 1/2 − [521]	34	25	11	12	7	2
589	588	5/2 1/2 − [521]	100	67	28	24	17	5
	598					4	4	2
680	681	11/2 11/2 − [505]	4	4	7	55	102	86
706	704	7/2 1/2 − [521]	202	136	62	32	26	16
746	743	3/2 3/2 + [402]	45	31	13	747	613	297
761		9/2 1/2 − [521]	25	18	21			
783	780	1/2 1/2 + [660]	33	13	4	265	195	77
	799					27	29	17
	816						17	17
837			3	8	4			
	855	9/2 1/2 + [660]				18	23	6
~ 875		5/2 5/2 − [512]		~ 3	~ 4			
	876					7	26	20
	924					12	13	3
950	945	7/2 5/2 − [512]	230	141	76	15	12	
977	973	1/2 1/2 + [400]	40	20	10	680	584	290
1000	999	3/2 1/2 + [660]	11	6	2	114	114	74
1044		9/2 5/2 − [512]	10		4			
*	1057	13/2 1/2 + [660]				43	52	49
	1077					13	15	
	1109	3/2 3/2 − [532]				85	54	33
	1126					46	26	7
	1143	3/2 1/2 − [530]				310	219	77
1138			234	103	59			

* Several unresolved (d,p) levels from 1044 keV to 1140 keV.

(continued)

TABLE 6 (continued).

Energy average (d,p) keV	Energy average (d,t) keV	Assignment	dσ/dΩ(d,p) μb/sr 60°	90°	125°	dσ/dΩ(d,t) μb/sr 60°	90°	125°
	1158	5/2 3/2 – [532]				115	90	28
	1176	5/2 1/2 – [530]				7	8	2
~ 1182		11/2 5/2 – [512]		~ 4	~ 5			
	1200					28	25	4
1204			24	15	18			
	1238	7/2 1/2 – [530] 7/2 3/2 – [532]				38	37	16
1237			23	8	9			
	1250					6	8	
	1282	7/2 1/2 + [660]				36	28	4
1287			31	16	7			
	1301	9/2 1/2 – [530]				10	13	4
	1341	9/2 3/2 – [532]				43	34	24
	1356					3	4	
	1390	11/2 1/2 – [530]				2	9	6
1396			49	28				
	1415					12		8
	1423					37		13
1430			157	78	28			
1474			18	10	5			
1493			31	19	9			
	1506					15		4
1521			104	39	15			
	1536					15		3
	1550					7		6
	1561					31		28
	1573					11		8
	1600					13	7	2
1602	**	3/2 1/2 – [510]	617	278	132			
1638		5/2 1/2 – [510]	171	92	45			
1693			135	60	70			
1718			41	22	18			
1751		7/2 1/2 – [510]	63	44	27			
1780			86	58	35			
1808			85	52	22			
	1810					9	7	
	1839					25	26	5
1840			53	26	16			
1887			86	39	21			

** Several unresolved (d,t) levels from 1600 keV to 1800 keV.

(continued)

TABLE 6 (continued).

Energy average		Assignment	$d\sigma/d\Omega(d,p)$ $\mu b/sr$			$d\sigma/d\Omega(d,t)$ $\mu b/sr$		
(d,p) keV	(d,t) keV		60°	90°	125°	60°	90°	125°
1909			29	18	13			
1925			71	32	15			
1953			79	25	18			
	1960	7/2 7/2 + [404]				98	104	95
1977		1/2 1/2 + [651]	265	131	37			
	1991					19	14	11
1993		3/2 1/2 + [651]	254	118	60			
2040		5/2 1/2 + [651]	320	154	28			
2053			86	74	80			
2081		7/2 1/2 + [651]	71	47	27			
2106			80	34	13			
2134			123	61	42			
2168			92	47	12			
2193			52	39	17			

4.2 General Features of the Spectra

As for the Yb nuclei, the basis for the interpretation of the (d,p) and (d,t) spectra has mostly been the systematic occurrence of characteristic intensity patterns for the rotational bands based on the different Nilsson states and the absolute cross sections for population of these bands. In many cases, this basis has been sufficient for a unique assignment but, as it will become evident from the discussion below, the spectra often show structures which in no simple manner can be accounted for by the Nilsson model. This is, of course, especially so for the nuclei which are not expected to have a stable equilibrium deformation, but also nuclei which possess all the characteristics of deformation show significant deviations from the expected scheme.

For the analysis of the more complicated cases, it has been of importance to utilize additional information, such as the rate of intensity change with angle, the cross sections for inelastic scattering, and the evidence available from decay scheme studies. Still, for a considerable number of levels, it has not been possible to give a satisfactory explanation.

This being the case, it is interesting to investigate whether the single-particle description is a sound basis for the analysis of the spectra. There

TABLE 7. Levels populated in ^{161}Gd.

Energy average (d,p) keV	Assignment	$d\sigma/d\Omega(d,p)$ $\mu b/sr$		
		60°	90°	125°
0	5/2 5/2 − [523]	30	20	8
73	7/2 5/2 − [523]	44	~ 20	11
163	9/2 5/2 − [523]	35	22	17
276	11/2 5/2 − [523]	12	7	6
313	3/2 3/2 − [521]	122	52	19
356	1/2 1/2 − [521]	387	168	57
397	3/2 1/2 − [521]	25	15	7
438	5/2 1/2 − [521]	313	195	87
510	7/2 3/2 − [521] 9/2 7/2 + [633]	33	24	10
529	7/2 1/2 − [521]	101	67	34
~ 585	11/2 7/2 + [633]	~ 2		~ 2
604	9/2 1/2 − [521]	23	13	11
645	11/2 3/2 − [521]	14	15	11
681	13/2 7/2 + [633]	48	51	38
~ 753	11/2 1/2 − [521]		~ 2	
~ 809	5/2 5/2 − [512]	10	~ 3	~ 2
834		188	82	32
889	7/2 5/2 − [512]	478		152
925		56	28	23
972	13/2 9/2 + [624]?	64	64	31
994	9/2 5/2 − [512]	9	16	12
1049		10	16	13
1097		12	9	7
1123	11/2 5/2 − [512]	7	11	8
1177		54	35	21
1309	1/2 1/2 − [510]	9	5	
1339	3/2 1/2 − [510]	538	300	
1378		192	79	
1403	5/2 1/2 − [510]	136	98	
1413		213	93	
1466	7/2 1/2 − [510]	77	46	29
1489	1/2 1/2 + [651]	242	157	48
1501	3/2 1/2 + [651]	151	137	59
1520		29	33	14
1556	5/2 1/2 + [651]	680	309	106
1591	7/2 1/2 + [651]	39	37	20
1615		91	50	16
1643		23	19	7
1664		46	27	14

TABLE 8. Q-values and neutron separation energies for Gd nuclei.

Mass A	$Q(d,t)$ A→A−1 keV	$Q(d,p)$ A−1→A keV	$S_n(d,t)$ keV	$S_n(d,p)$ keV
152	−2338 ± 10		8596 ± 10	
153		4015 ± 10		6240 ± 10
154	−2642 ± 10		8900 ± 10	
155	−190 ± 10	4217 ± 10	6448 ± 10	6442 ± 10
156	−2287 ± 10	6319 ± 10	8545 ± 10	8544 ± 10
157	−112 ± 10	4136 ± 10	6370 ± 10	6361 ± 10
158	−1688 ± 10	5724 ± 10	7946 ± 10	7949 ± 10
159		3717 ± 10		5942 ± 10
160	−1200 ± 10		7458 ± 10	
161		3411 ± 10		5636 ± 10

is ample evidence for a considerable spreading of intensity, and it is not easy to see how distant single-particle levels one should consider in the analysis. Some light might be shed on this problem by the size of the integrated cross section for all levels in the low energy spectrum.

Let us first consider the levels populated by the (d,t) reaction. In the deformed nuclei ^{159}Gd, ^{157}Gd, and ^{155}Gd, the level assigned as $7/2+[404]$ gives a natural limit for the summation of cross sections. A possibly related level in ^{153}Gd is found at 1287 keV and the summation can be carried to this energy. For experimental reasons, the (d,t) spectrum in ^{151}Gd was not recorded above 1400 keV. The summed cross sections with these limits are plotted in fig. 3 as a function of the mass number. All cross sections have been reduced to $Q = -2$ MeV, as explained in sect. 2. For the deformed nuclei, there is surprisingly good agreement between the experimental cross sections and the summed theoretical cross sections for all Nilsson levels from the $7/2+[404]$ level to the $3/2-[521]$ level. The latter is ground state in three of the nuclei and can therefore be assumed to represent the Fermi surface. Although this agreement may be fortuitous, it is indicated that the expected strength for the hole states by and large is observed. The total (d,t) cross section is only about half that expected for a pure shell model including the $N = 4$ $g_{7/2}$, $s_{1/2}$, and $d_{3/2}$ levels, the $N = 5$ $h_{11/2}$ levels and half of the $N = 5$ $f_{7/2}$ levels.

A similar comparison for the (d,p) cross sections is considerably more uncertain because of the lack of suitable summation limits. Fig. 3 shows the summed (d,p) cross section between the ground state and a somewhat

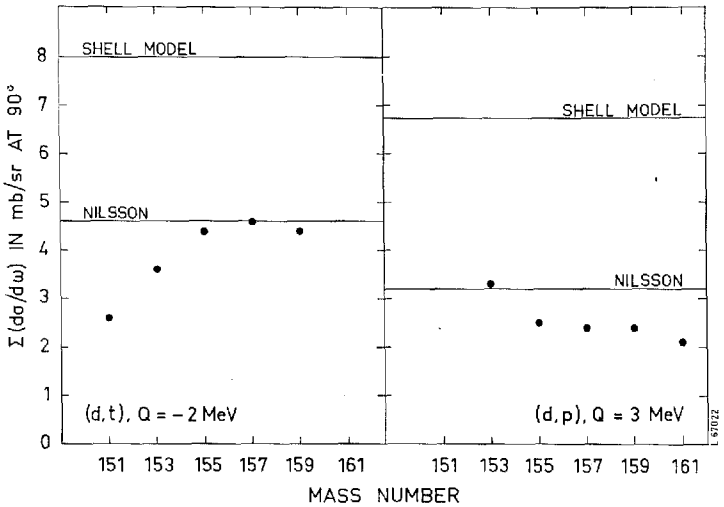

Fig. 3. Summed cross section as a function of the mass number.

arbitrarily chosen limit at 2 MeV of excitation. The theoretical Nilsson cross section sum from the $3/2-[521]$ orbital to the $1/2+[651]$ orbital is in reasonably good agreement with the experimental sum. The increase in the summed cross section for ^{153}Gd probably reflects the lowering of the states as the spherical shell-model configurations are approached.

A comparison can also be made for the densities of levels observed in the transfer reactions. Couplings between the individual single-particle levels as, e.g., the Coriolis coupling will redistribute the intensities. This will not greatly affect the number of levels observed in the spectrum although, in some cases, a weakly populated level in one band can get admixtures of a strongly populated level in another band and thereby contribute to the observed level density. Couplings of the single-particle states to the vibrational states will increase the number of levels populated compared to what is predicted from the Nilsson scheme. Fig. 4 shows the results of a comparison of this type for the levels in the Gd nuclei. The energy regions included are the same as those used for the comparison of cross sections in fig. 3. The moderate increase in level density indicates that the number of levels strongly coupled to additional degrees of freedom (vibrations) is rather small.

4.3. Detailed Interpretation of the Spectra

This section contains a detailed discussion of the features of the spectra, which it has been possible to describe in terms of single-particle levels in a deformed well and the couplings of such levels to each other or to elementary

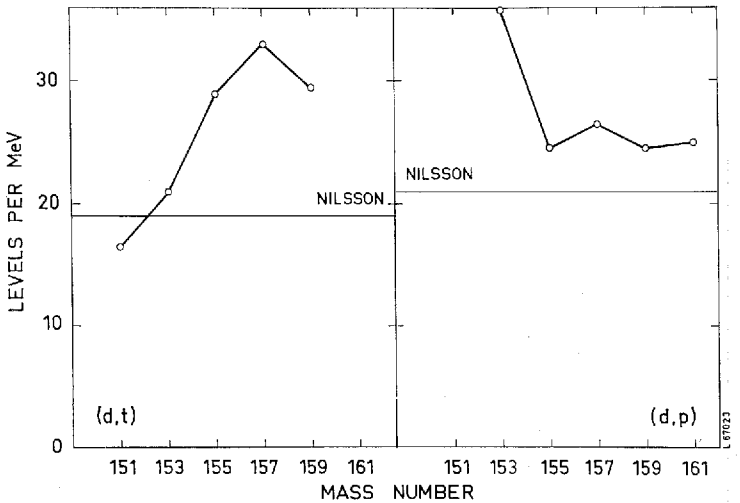

Fig. 4. The density of levels as a function of the mass number.

vibrational modes. The individual Nilsson orbits are discussed separately below. Tables 9 and 10 list the theoretical cross sections for the (d,t) and (d,p) reactions, respectively, for the pure single-particle states. The observed energies of the band heads are plotted in fig. 15, and the complete level schemes for the six nuclei investigated are shown in figs. 16–21.

4.3.1. The 3/2–[521] Orbital

This orbital is the ground state in ^{155}Gd, ^{157}Gd, and ^{159}Gd. In ^{161}Gd, a group at 313 keV has a cross section and angular dependence as expected for the $3/2-$ level of this band. The $7/2-$ state, however, must then coincide with the assigned $5/2\ 1/2-[521]$ state and the $9/2-$ state with the $7/2\ 1/2-[521]$ state. A possible $11/2-$ state is then observed at 645 keV.

The $3/2-$, $7/2-$, $9/2-$, and $11/2-$ members of the band are all observed in the three nuclei where this band occurs as ground state, except in ^{155}Gd where the $11/2-$ member coincides with another group. The intensities are roughly in agreement with those given in table 9. The $5/2-$ member of the band, which is not expected to be observed for the pure Nilsson state, is weakly populated in the bands considered here. This may be mostly a result of the Coriolis coupling to the $5/2-[523]$ band and will be discussed later.

The occurrence of the same band as ground state in three consecutive nuclei is a somewhat remarkable fact which must be associated with the crossings of the $3/2+[651]$ and $5/2+[642]$ states with the $3/2-[521]$ state. The considerable change in deformation with increasing neutron number is

TABLE 9. The theoretical cross sections in $\mu b/sr$ for (d,t) reactions in the Gd isotopes.

$Q = -2\,\mathrm{MeV}$, $\theta = 90°$, $V^2 = 1$.

J Nilsson orbital	1/2	3/2	5/2	7/2	9/2	11/2	13/2
1/2+[411]	126	336	154	36	6	–	–
5/2+[402]	–	–	71	12	5	–	–
7/2+[404]	–	–	–	157	3	–	–
1/2+[400]	858	189	90	6	1	–	–
3/2+[402]	–	678	56	12	1	–	–
1/2−[541]	183	233	171	24	25	14	–
7/2−[523]	–	–	–	20	2	89	–
1/2−[530]	10	357	35	137	30	14	–
1/2+[660]	12	4	81	1	104	0	27
3/2−[532]	–	65	126	48	53	10	–
3/2+[651]	–	1	32	2	83	0.4	33
9/2−[514]	–	–	–	–	1	93	–
5/2+[642]	–	–	6	1	55	0.6	37
3/2−[521]	–	176	~0	315	24	11	–
5/2−[523]	–	–	44	45	74	6	–
11/2−[505]	–	–	–	–	–	94	–
1/2−[521]	420	41	108	147	25	4	–
7/2+[633]	–	–	–	0.5	28	0.7	40
1/2+[651]	171	195	249	92	24	9	6
5/2−[512]	–	–	6	465	13	6	–
7/2−[514]	–	–	–	26	87	3	–

apparently large enough to ensure that the 3/2−[521] state stays above the two $N = 6$ states (see fig. 23). This seems to require that the crossings of the energy levels occurs at somewhat larger deformation than indicated by the newest Nilsson diagrams[18].

The (d,t) cross sections for the 3/2− and 7/2− states, which are plotted in fig. 22, clearly show the increased filling of the 3/2−[521] orbital as the neutron number is increased. A corresponding variation can be traced in the (d,p) cross sections, but the behaviour is less regular.

The moments of inertia for the 3/2−[521] bands are listed in table 11. It should be remarked that the rotational energies of this band show an alternating energy term similar to that observed in the ^{159}Tb spectrum[19]. The analysis of the rotational energies will be published later[8].

TABLE 10. The theoretical cross sections in $\mu b/sr$ for (d,p) reactions in the Gd isotopes.

$Q = +3\,\mathrm{MeV}$, $\theta = 90°$, $U^2 = 1$.

J Nilsson orbital	1/2	3/2	5/2	7/2	9/2	11/2	13/2
11/2 − [505]	–	–	–	–	–	69	–
3/2 + [651]	–	1	23	1	78	0.4	34
3/2 − [521]	–	107	~0	275	17	8	–
5/2 + [642]	–	–	4	1	39	0.6	37
5/2 − [523]	–	–	39	40	54	4	–
1/2 − [521]	255	25	95	120	18	3	–
7/2 + [633]	–	–	–	0.3	20	0.7	40
1/2 + [651]	120	137	171	65	16	10	6
5/2 − [512]	–	–	5	408	10	4	–
7/2 − [503]	–	–	–	482	4	2	–
7/2 − [514]	–	–	–	22	63	2	–
9/2 + [624]	–	–	–	–	6	0.6	42
1/2 + [640]	52	3	210	34	49	15	5
3/2 + [642]	–	29	83	67	9	20	5
1/2 − [510]	10	414	151	100	6	1	–
3/2 − [512]	–	82	333	62	10	0.8	–
3/2 − [501]	–	784	72	40	~1	~0	–

4.3.2. The 5/2 + [642] and the 3/2 + [651] Orbitals

The identification of the 5/2 + [642] orbital in the deformed Gd nuclei is somewhat doubtful. The predicted pattern consists of two lines with $j = 9/2$ and $j = 13/2$, respectively. A similar pattern is expected for the 3/2 + [651] orbital where the 5/2 + state, however, is also populated (cf. tables 9 and 10). The situation is further complicated by the strong Coriolis matrix element between these two bands and by the abnormal order of filling of the Nilsson orbitals. The latter is illustrated in fig. 23, which is drawn to explain the persistent occurrence of the 3/2 − [521] state as ground state in the Gd nuclei.

With the reservations necessitated by the complications discussed above, plausible 5/2 + [642] bands have been found in the ^{159}Gd and ^{157}Gd nuclei. The assignment in ^{157}Gd is in agreement with earlier decay scheme work. For ^{159}Gd, the (d,t) spectrum is relatively clear in the region of the band proposed and the study of the angular distributions supports the assignments[7].

In ^{155}Gd, the 5/2 + level at 105 keV which has been proposed for the 5/2 5/2 + [642] level[11,20] is strongly populated in both the (d,p) and the

TABLE 11. Inertial parameters and decoupling parameters. Numbers in brackets are decoupling parameters for $K = 1/2$ bands.

Nilsson orbital	161	159	157	155	153
3/2 − [521]	10.4	10.0	11.0	12.0	
5/2 − [523]	10.3	11.5	11.8	10.2	
5/2 + [642]		7.7	7.5		
1/2 + [660]		13.3 (4.51)			
3/2 − [532]		9.8	10.2		
1/2 − [530]		7.7 (0.15)	7.7 (0.16)	8.6 (0.12)	
1/2 − [521]	10.9 (0.25)	11.6 (0.49)	12.2 (0.27)	13.9 (0.32)	16.0 (0.74)
7/2 + [633]	7.1				
5/2 − [512]	11.5	10.7			
1/2 − [510]	11.3 (−0.12)	11.6 (0.38)			
1/2 + [651]	7.6 (−0.47)	7.3 (−0.27)			

(d, t) reactions and can therefore not be the band head of the 5/2 + [642] orbital, unless this orbital is heavily mixed with orbitals which have strong components of $j\pi = 5/2+$. Inspection of table 9 shows that such components are found for the 1/2 + [400], 3/2 + [402], 1/2 + [660], and 3/2 + [651] orbitals which all are expected as low lying states in the Gd nuclei. However, the (d, t) cross section for the 106 keV level is considerably larger than expected for any 5/2 + component and a 5/2 + assignment is therefore untenable. A more likely explanation for the 106 keV level is that it represents a fraction ($\sim$40 %) of the strong 3/2 3/2 + [402] state. A splitting of this intensity could result from the coupling of the 3/2 + [651] and the 3/2 + [402] levels which are expected to cross for deformations $\delta \sim 0.3$. A similar phenomenon is discussed in sect. 4.3.3 for the 1/2 + [660] orbital. If indeed the 106 keV is a 3/2 + level related to the 3/2 + [651] orbital, it is reasonable to suggest that the level at 86 keV seen in the decay studies[20], which is weakly populated in the transfer reactions, is a 5/2 + level related to the 5/2 + [642] orbital. This would be consistent with all the information available. Furthermore, the angular distribution for the level at 214 keV is similar to that observed for the 13/2 5/2 + [642] level in ^{159}Gd and is therefore possibly the 13/2 + level of this or the 3/2 + [651] band. Unfortunately, this observation does not make the structures of these strongly Coriolis mixed bands in ^{155}Gd much clearer. Further mixing is caused by the large Coriolis matrix elements which connect several of the positive parity states mentioned above. It is exceedingly difficult to comprehend the result of the simultaneous operation of all the couplings, and it is therefore not surprising that it has been impossible to

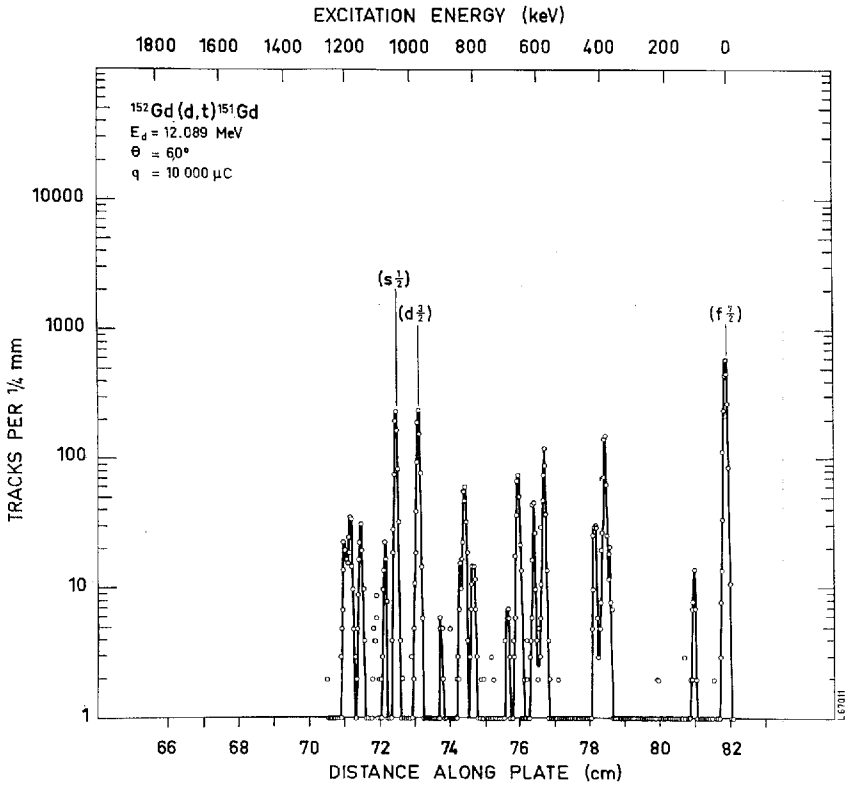

Fig. 5. Triton spectrum for the reaction ^{152}Gd$(d,t)^{151}$Gd $\theta = 60°$.

identify with certainty the $3/2+[651]$ band in any of the Gd nuclei, although this band is expected to occur at quite low excitation energies.

It should be remarked that the occurrence of crossing energy levels in the Gd nuclei is intimately connected with the onset of deformation, and a discussion of the resulting coupling phenomena is of interest for our whole understanding of the Nilsson model. We therefore plan to return to this problem which can be attacked, partly, by improvements in the experimental material and, partly, by the construction of computer programmes which allow a rapid evaluation of the expected energy levels and their population by the transfer reactions. An angular distribution study for the ^{156}Gd(d,t) ^{155}Gd reaction which presently is being analyzed[21] could add considerably to our understanding of the crucial ^{155}Gd spectrum.

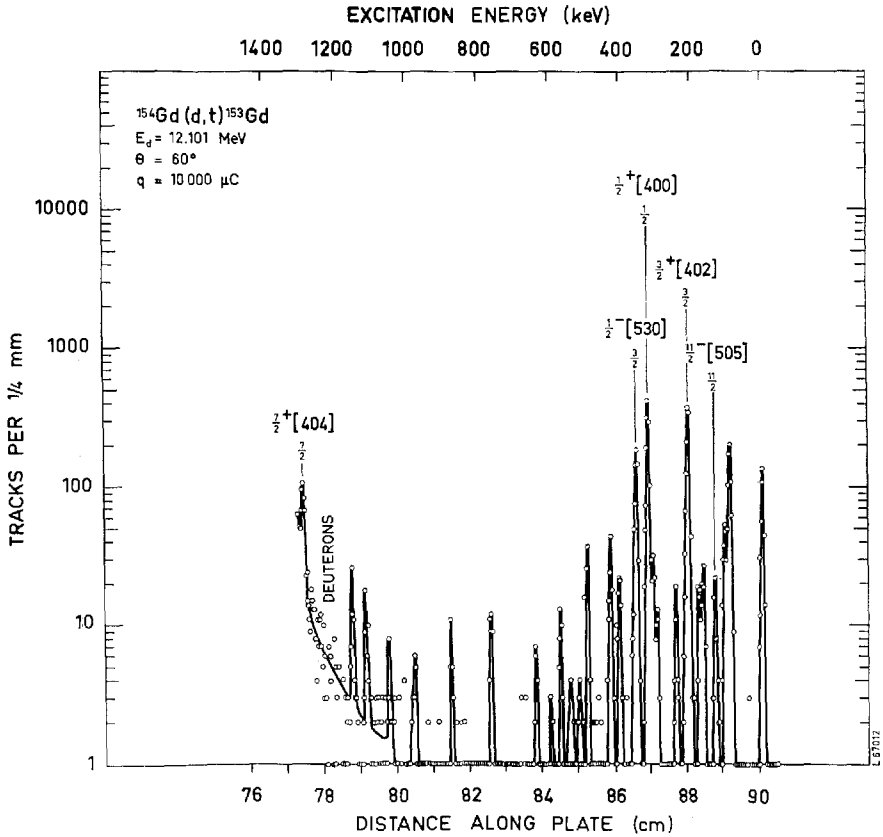

Fig. 6. Triton spectrum for the reaction $^{154}Gd(d,t)^{153}Gd$ $\theta = 60°$.

4.3.3. The 1/2 + [660] Orbital

The $^{160}Gd(d,t)^{159}Gd$ spectrum has a strong group corresponding to a level energy of 780 keV. The angular distribution for this group[7] strongly suggests $l = 0$. Apart from that of the 1/2 1/2 + [400] level, no strong $l = 0$ groups are expected and the only reasonable explanation for the 780 keV group is that it represents a fraction of the 1/2 1/2 + [400] intensity, the bulk of which is found in the group at 973 keV (cf. sect. 4.3.5). A possible mechanism for such a splitting of intensity is the coupling between the orbitals 1/2 + [660] and 1/2 + [400] which, as discussed above, are expected to cross each other.

The theoretical decoupling parameter of the 1/2 + [660] band is $a = 6.0$, and it is interesting that it has been possible (cf. fig. 20) to construct a band of levels with reasonable intensities and l-values, which corresponds to

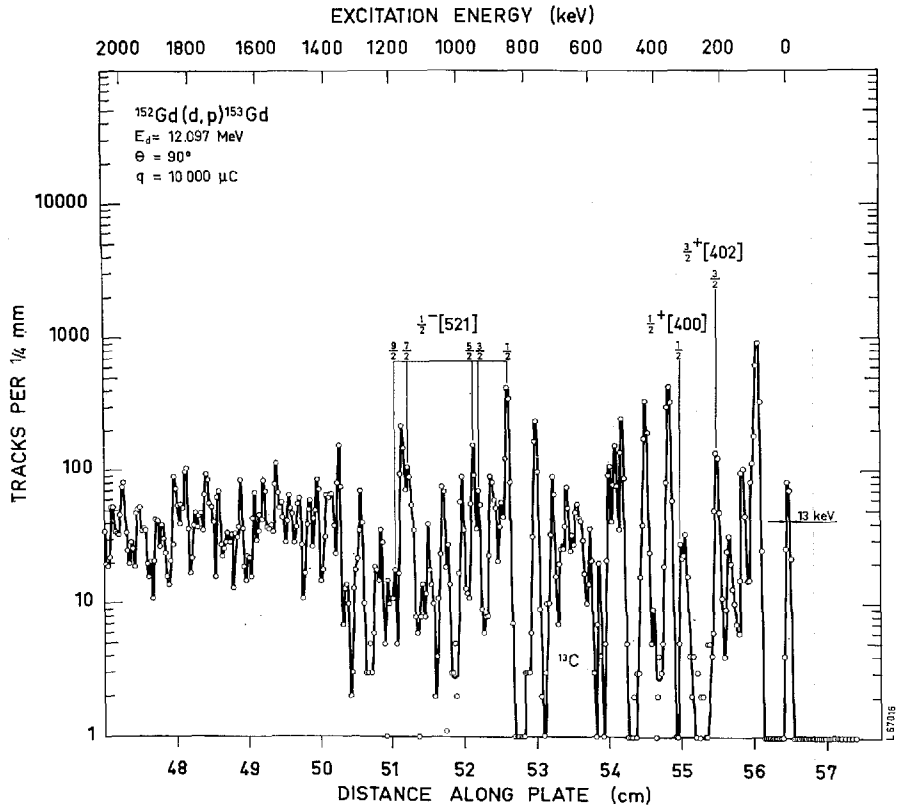

Fig. 7. Proton spectrum for the reaction ^{152}Gd$(d,p)^{153}$Gd $\theta = 90°$. In this and in the following figures, groups ascribed to reactions on target impurities are indicated by the symbol of the impurity. Thus, the broad group marked ^{13}C is due to the ^{13}C$(d,p)^{14}$C reaction.

$a = 4.51$ and $A = 13.3$ keV. Unfortunately, there are several other solutions with the same $1/2+$ and $13/2+$ states as shown in fig. 20. Nevertheless, this identification is the most convincing observation of the $1/2+[660]$ orbital made up to now.

4.3.4. The 11/2–[505] Orbital

Only the $11/2-$ member of this band is expected to be populated in the transfer reactions. Still, it has been possible to identify this orbital in ^{159}Gd, ^{157}Gd, ^{155}Gd, and ^{153}Gd on the basis of the characteristic angular dependence of the $l = 5$ transitions. Furthermore, an isomer in ^{157}Gd has been observed[22] at 423 keV, which is in agreement with the energy of the $11/2-$ level observed here.

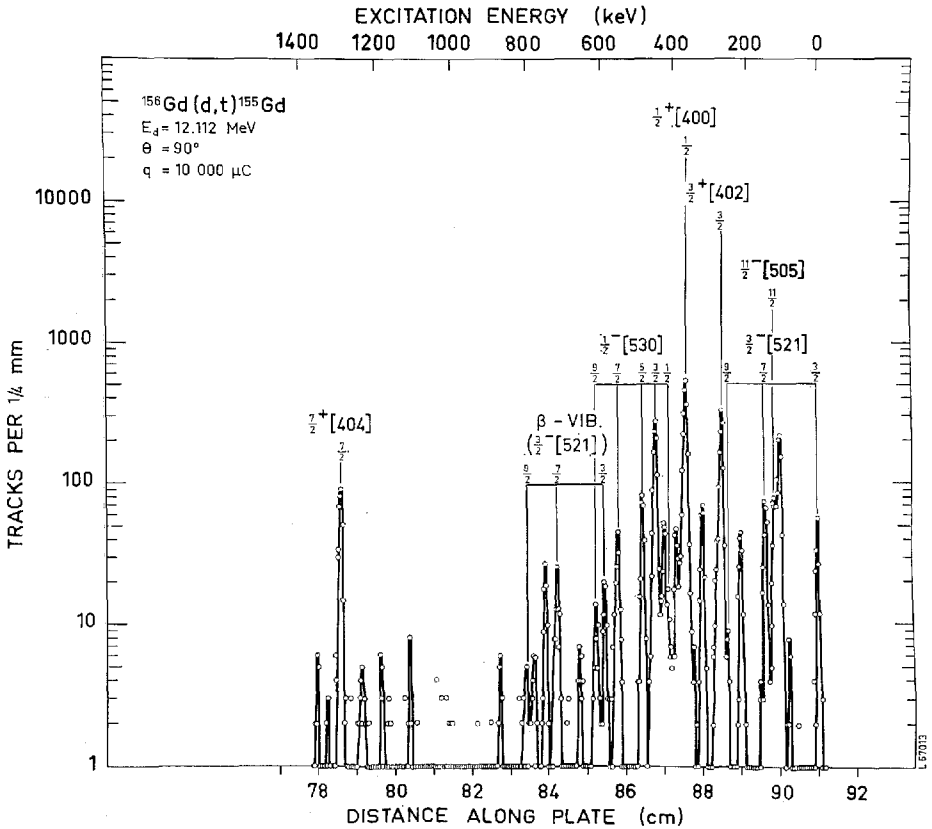

Fig. 8. Triton spectrum for the reaction ^{156}Gd$(d,t)^{155}$Gd $\theta = 90°$.

In ^{155}Gd, the levels at 119 keV and 214 keV are possible candidates for a $11/2-[505]$ assignment. Recent angular distribution measurements[21] slightly favour the 119 keV level for the $11/2-[505]$ assignment, but this level can then hardly be identical to a known level[20] at 118 keV. A possible explanation for the 214 keV level was discussed in sect. 4.3.2.

For the above mentioned nuclei, the ratios of the triton intensities at 90°, $Q = -2$ MeV to the calculated intensities are 1.02, 0.79, 1.27, and 0.51, respectively, which indicates a slowly decreasing filling of this orbital as the neutron number is reduced. In ^{159}Gd and ^{157}Gd, the level is weakly populated in the (d,p) reaction (cf. tables 6 and 5), as expected for a hole state. In ^{155}Gd and ^{153}Gd, somewhat stronger (d,p) groups occur at the positions for the $11/2-$ levels. The excitation energy for this orbital shows a smooth dependence on the neutron number (fig. 15).

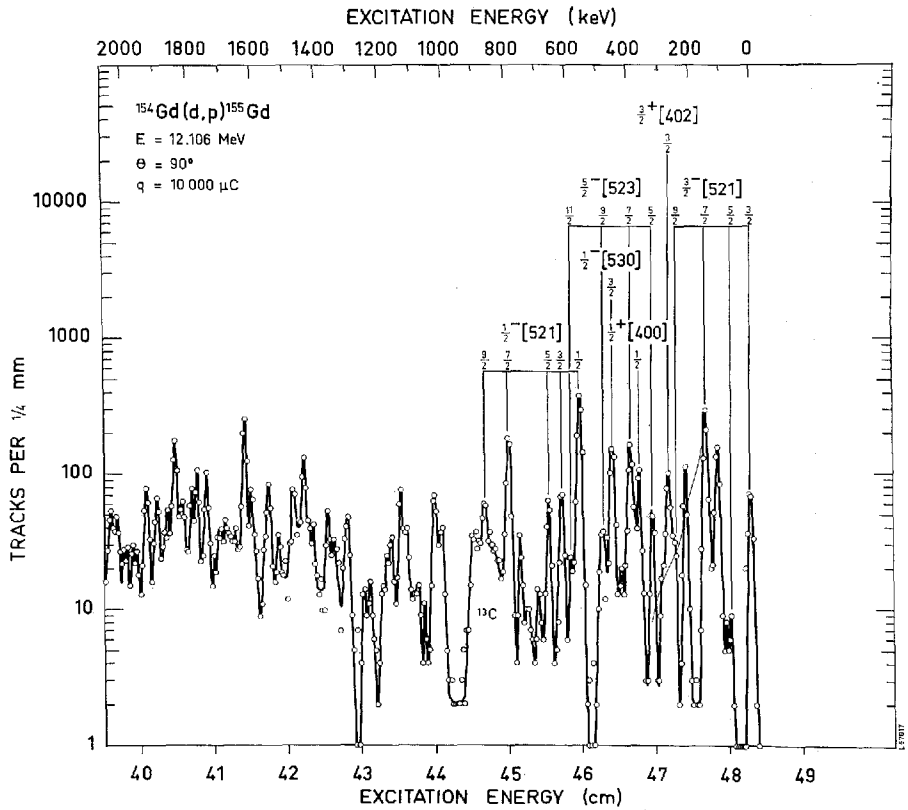

Fig. 9. Proton spectrum for the reaction ^{154}Gd$(d,p)^{155}$Gd $\theta = 90°$.

4.3.5. The 3/2 + [402] and the 1/2 + [400] Orbitals

Table 9 shows that very strong lines are expected in the (d,t) spectra from the $3/2+[402]$ and the $1/2+[400]$ orbitals which originate in the $d_{3/2}$ and $s_{1/2}$ shell model states. Indeed, all the (d,t) spectra show two strong lines fairly close to each other, which could be the $3/2+$ and $1/2+$ states of these bands, but it has been difficult to decide which group belongs to which orbital and, in all cases, one must accept considerable deviations between the theoretical rotational patterns and those observed. For a general discussion of the various coupling phenomena which could cause such deviations see sect. 4.3.2.

In the ^{159}Gd spectrum the angular distributions[7] unambiguously show that the group at 734 keV has $l = 2$, whereas the group at 973 keV has $l = 0$. In view of the large cross sections for these lines, the assignments to the

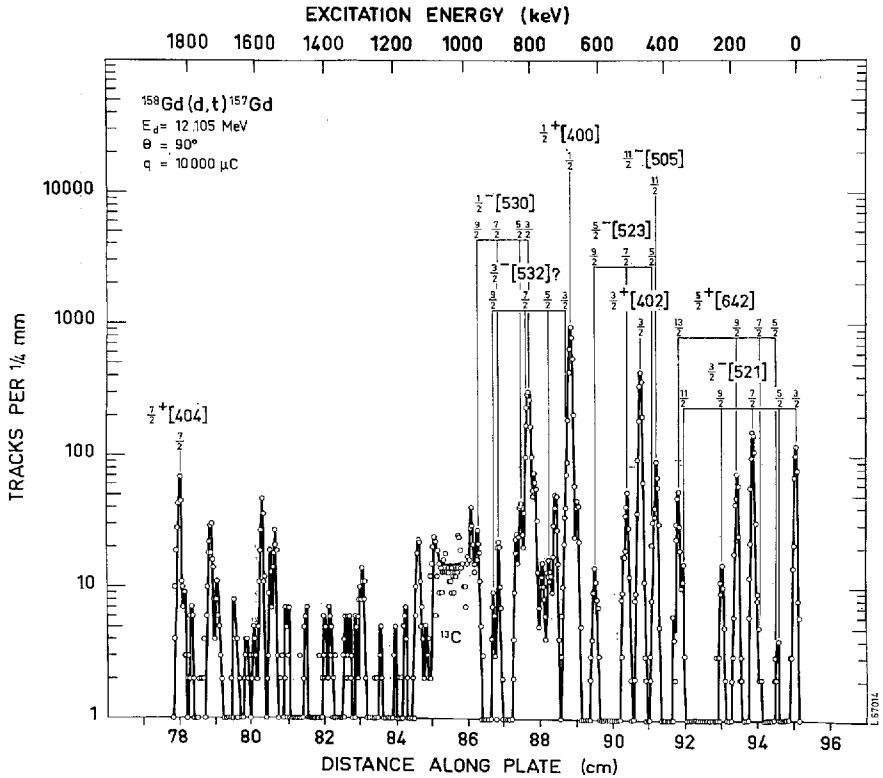

Fig. 10. Triton spectrum for the reaction ^{158}Gd$(d,t)^{157}$Gd $\theta = 90°$.

states 3/2 3/2 + [402] and 1/2 1/2 + [400], respectively, are certain. The level order is then in agreement with that of the Nilsson model[2]. The same level order has then been assumed for the deformed nuclei ^{157}Gd, ^{155}Gd, and ^{153}Gd. In the ^{151}Gd spectrum, there are two strong lines at 977 keV and 1047 keV. Although the nature of these states is not clear, it is natural to assume that they contain large components of the $d_{3/2}$ and $s_{1/2}$ shell-model states, respectively.

As mentioned above, there are considerable difficulties connected with the assignment of rotational bands for the $N = 4$ states. Table 9 shows that the 3/2 + and 5/2 + states in the 1/2 + [400] band and the 5/2 + state in the 3/2 + [402] band are expected to have appreciable (d,t) cross sections. Again, the ^{159}Gd spectrum is the most favourable case to discuss. As mentioned in sect. 4.3.3, the level at 780 keV seems to be populated mainly by $l = 0$ and can therefore not to any appreciable extent be the 5/2 + state of the

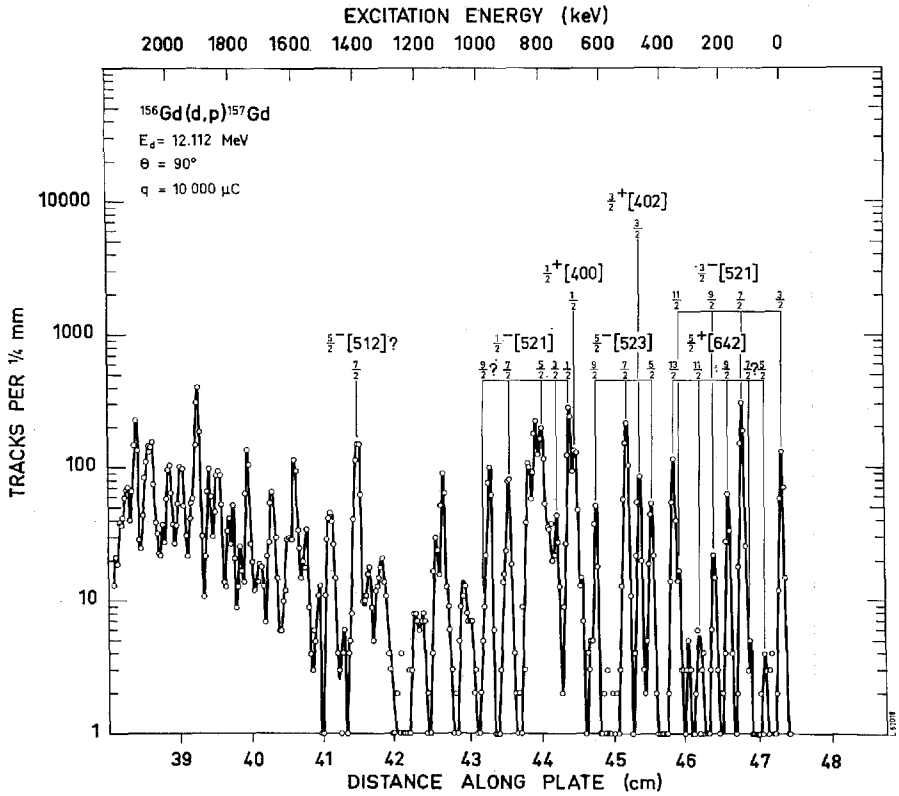

Fig. 11. Proton spectrum for the reaction ^{156}Gd$(d,p)^{157}$Gd $\theta = 90°$.

3/2 + [402] band. Such an assignment would also imply a very large moment of inertia for this band. The group at 799 keV could possibly represent the 5/2 + state which would correspond to an inertial parameter $A = 11.2$ keV, but the intensity is less than expected and the data on the angular distribution, although inconclusive, does not support an $l = 2$ assignment. In ^{157}Gd, the 513 keV group has about the right intensity for the 5/2 + level. The inertial parameter would then be $A = 7.6$ keV. A similar group is observed at 322 keV in ^{155}Gd which implies $A = 11.0$ keV, but again the evidence for a 5/2 + assignment is meager.

The situation with respect to the 3/2 + and 5/2 + states in the 1/2 + [400] band is even less clear. In ^{159}Gd, the 999 keV group has an $l = 2$ angular distribution and also the absolute cross section is as expected for the 3/2 + state. However, the only group which could correspond to the 5/2 + state

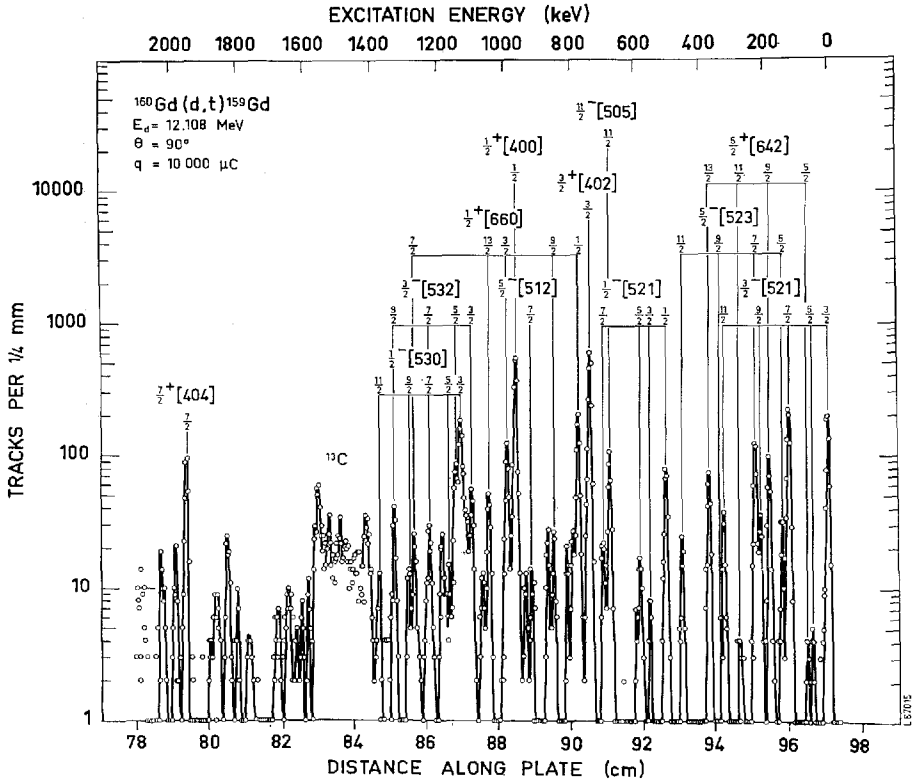

Fig. 12. Triton spectrum for the reaction ^{160}Gd$(d,t)^{159}$Gd $\theta = 90°$.

is then at 1057 keV, but this group has an angular distribution which indicates a high angular momentum, possibly $l = 6$. This group is tentatively assigned to the $13/2+$ member of the $1/2+[660]$ band (cf. sect. 4.3.3), but could of course contain some contribution from the $5/2$ $1/2+[400]$ state. If this is the case, the parameters for this band are $a = -0.15$ and $A = 10.0$ keV. This is somewhat surprising as the pure band is expected to have a slightly positive decoupling parameter. Also the admixture of the $1/2+[660]$ band indicated by the intensity of the state assigned $1/2$ $1/2+[660]$ would yield a large positive decoupling parameter.

The other Gd nuclei show no structures which can be ascribed to simple rotational bands based on the $1/2+[400]$ state.

4.3.6. The 3/2–[532] Orbital

This orbital is expected to occur as a hole state between the $1/2+[400]$ orbital and the $1/2-[530]$ orbital to be discussed in the following section.

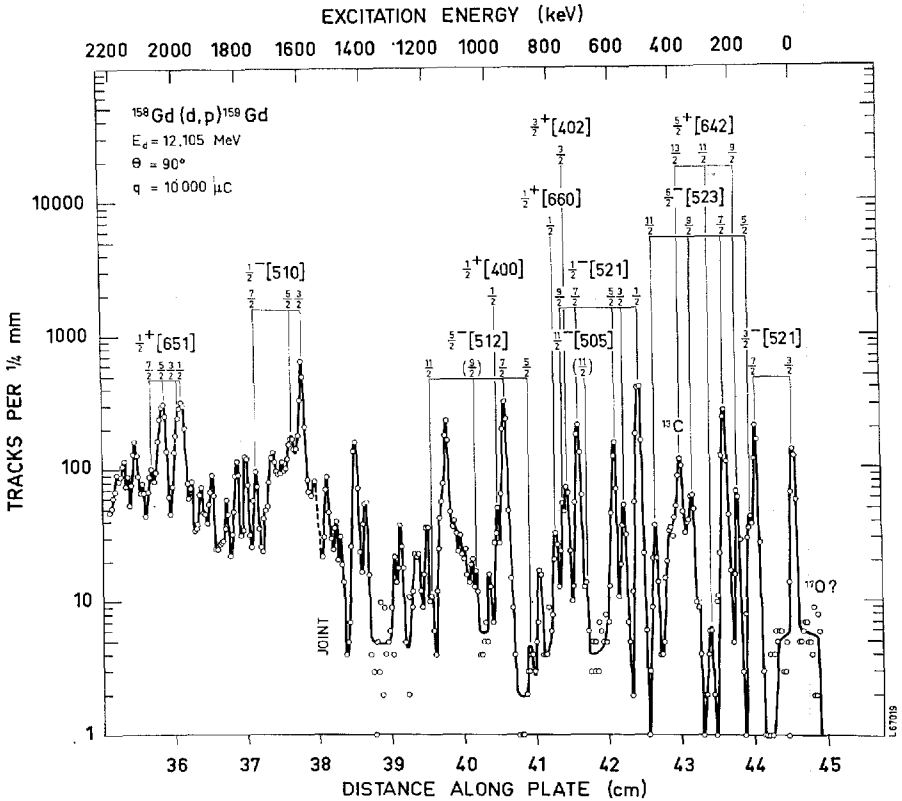

Fig. 13. Proton spectrum for the reaction ^{158}Gd$(d,p)^{159}$Gd $\theta = 90°$.

The pattern consists of rather strongly populated 3/2, 5/2, 7/2, and 9/2 levels and a somewhat weaker 11/2 level. Some deviations from the pattern can be expected because of couplings to the large number of $K\pi = 1/2-$ and $3/2-$ bands in this region of the Nilsson diagram.

In ^{159}Gd, the $3/2-$ level has been placed at 1109 keV where a group with $l = 1$ is observed[7]. The intensities of the rotational states agree well with the theoretical intensities, but the rotational spacings are somewhat irregular. In ^{157}Gd, there are several possible positions for the $3/2-[532]$ band, the most likely being the one indicated in fig. 19. The intensities are, however, not in good agreement with those calculated and again the rotational spacings show some deviations. The band has not been identified in ^{155}Gd.

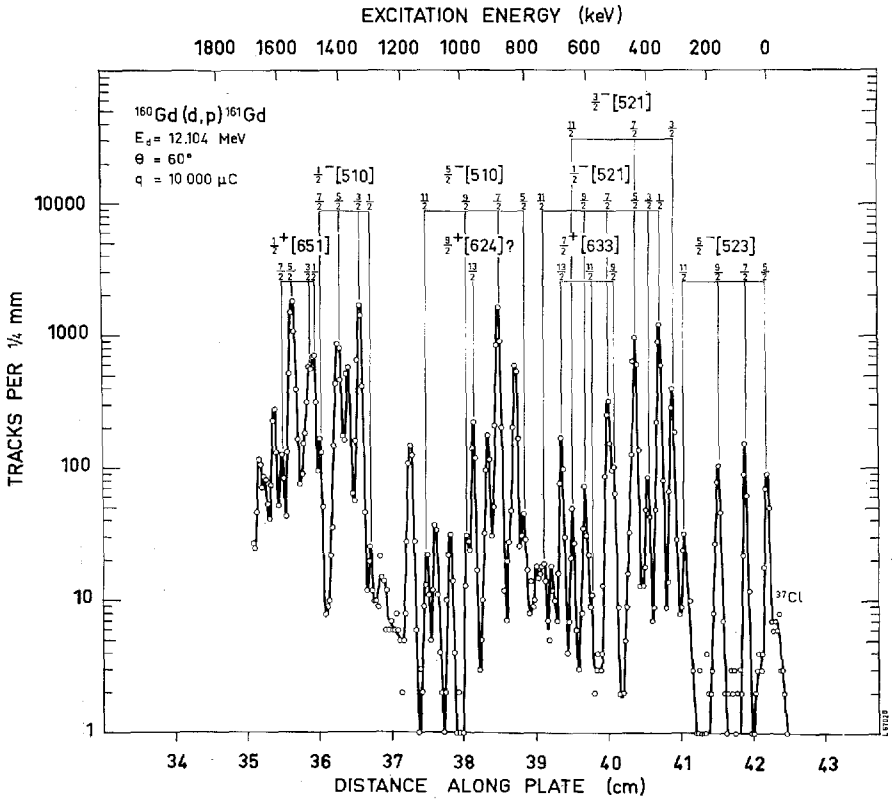

Fig. 14. Proton spectrum for the reaction ^{160}Gd$(d,p)^{161}$Gd $\theta = 60°$.

4.3.7. The 1/2–[530] Orbital

The $1/2-[530]$ orbital is characterized by a strong population in the (d,t) reaction of the $3/2-$ state and a somewhat smaller population of the $7/2-$ state. The theoretical decoupling parameter is $a = -0.31$, but this value is quite sensitive to changes in the deformation.

For all the Gd nuclei, a strong group is observed in the (d,t) spectra at an excitation energy slightly higher than that of the $1/2+[400]$ orbital. In ^{159}Gd, this group occurs at 1143 keV and has an $l = 1, j = 3/2$ distribution[7]. The assignment $3/2\ 1/2-[530]$ is therefore quite certain, but there are several possibilities for the associated rotational band. The band shown in fig. 20 corresponds to $a = 0.15$ and $A = 7.7$ keV. The intensities are in good agreement with those calculated from the theoretical wave functions, except for the $7/2-$ state where the observed intensity is less than $50\,\%$ of the

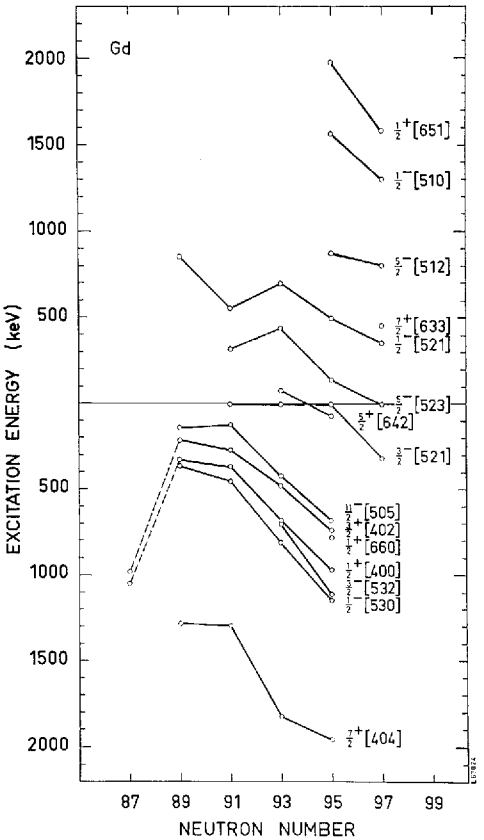

Fig. 15. Energies of the band heads for the Nilsson states observed. Points at negative energies indicate hole states.

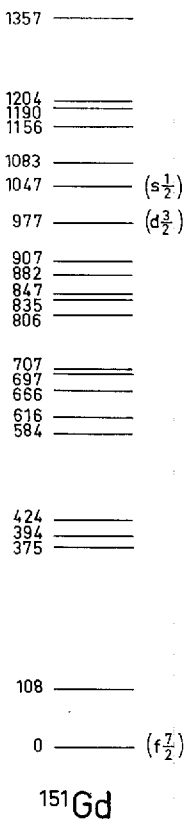

Fig. 16. Level scheme for ^{151}Gd.

calculated intensity. This discrepancy is furthermore increased, because the state assigned as 7/2 3/2 − [532] within the experimental resolution occurs at the same energy. The only other possible choice for the 7/2 1/2 − [530] group is that at 1282 keV which, however, has only about 30 % of the theoretical cross section. The 5/2 − and 9/2 − groups could then be those at 1200 keV and 1390 keV, which yields $a = 0.014$ and $A = 11.6$ keV. A closer analysis including the effects of the Coriolis coupling to several nearby bands is necessary to choose between the bands proposed, but the one given in fig. 20 may be preferable because of its similarity to the 1/2 − [530] bands suggested in ^{157}Gd and ^{155}Gd.

In ^{157}Gd, the 3/2 − state is undoubtedly found at 809 keV. The band sug-

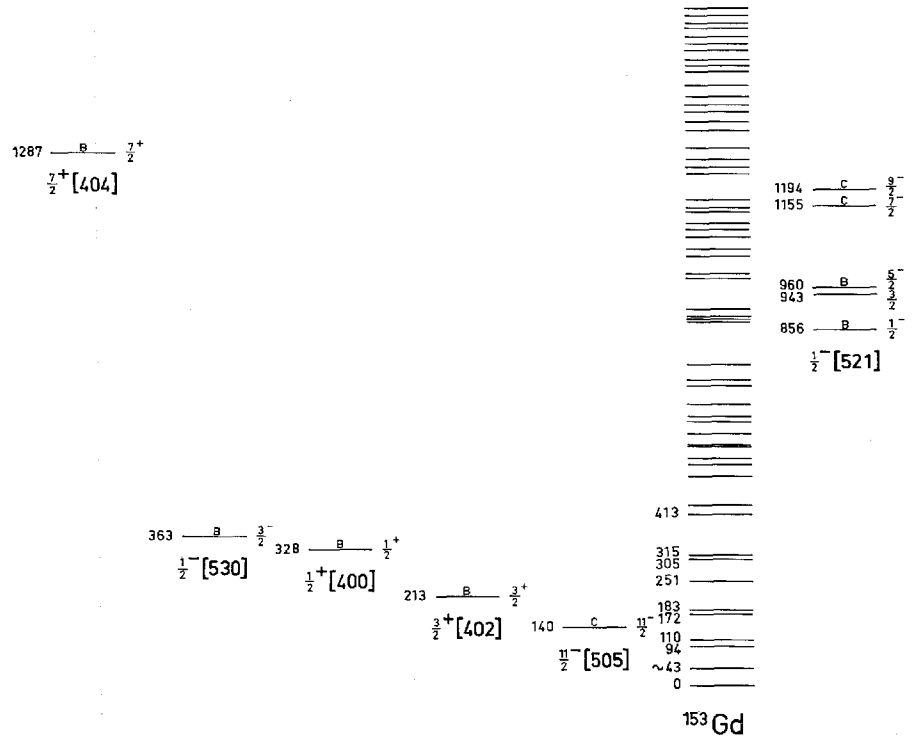

Fig. 17. Level scheme for ^{153}Gd. Nilsson states to the left are hole excitations, those to the right particle excitations. The letter *A* indicates that all the available data suggest the assignment, *B* an assignment consistent with the observations, but where lack of resolution or intensity prevents a definite assignment. Finally, *C* indicates that a group was observed at the position expected, e.g., for a rotational level but with an intensity considerably different from the theoretically predicted intensity.

gested in fig. 19 yields $a = 0.16$ and $A = 7.7$ keV, but, as it was the case in ^{159}Gd, the intensity of the $7/2-$ state is weaker than expected, whereas the $5/2-$ state is too strong. In ^{155}Gd, the $3/2-$ state is found at 451 keV, and an acceptable band with $a = 0.12$ and $A = 8.6$ keV is shown in fig. 18. Also here the $7/2-$ intensity is too weak and the $5/2-$ intensity too large. The group at 426 keV could correspond to the $1/2-$ state of this band. The band is excited quite strongly in the (d, d') reaction, which indicates a Coriolis coupling to the $3/2-[521]$ ground-state band[8].

In ^{153}Gd, the group at 363 keV is probably related to the $3/2$ $1/2-[530]$ states in the nuclei discussed above. The groups at 436 keV and 504 keV can be incorporated as $5/2-$ and $7/2-$ states in a band with $a = -0.2$ and $A = 12.2$ keV, but the existence of rotational spectra in this nucleus is by no means well established.

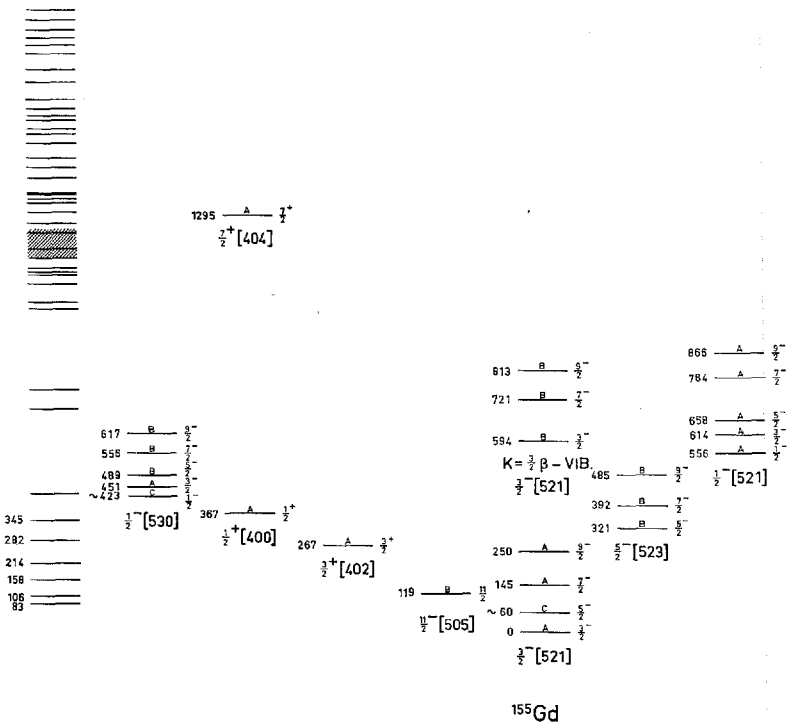

Fig. 18. Level scheme for ^{155}Gd.

The (d,t) spectra for ^{151}Gd do not show any strong groups immediately above those which, in sect. 4.3.5, were related to the $d_{3/2}$ and $s_{1/2}$ shell model states. It is possible that most of the strength, which in the deformed nuclei went into the $1/2-[530]$ band, in ^{151}Gd occurs at lower excitation energy than the $N = 4$ states do.

4.3.8. The 7/2 + [404] Orbital

The $7/2+[404]$ orbital is expected to occur as the next hole state after the $1/2-[530]$ state. Only the $7/2+$ member has an appreciable (d,t) cross section. In agreement with this expectation, the (d,t) spectra of ^{159}Gd, ^{157}Gd, ^{155}Gd, and ^{153}Gd show a single strong line at an excitation energy between 2.0 MeV and 1.3 MeV. For ^{151}Gd, the relevant part of the spectrum was obscured by deuterons. The angular distribution for the line in the ^{159}Gd spectrum is in good agreement with an $l = 4$ assignment, and the angular intensity variation for the group in the ^{157}Gd and ^{155}Gd spectra followed the same pattern. The assignment to the $7/2+[404]$ orbital is therefore quite

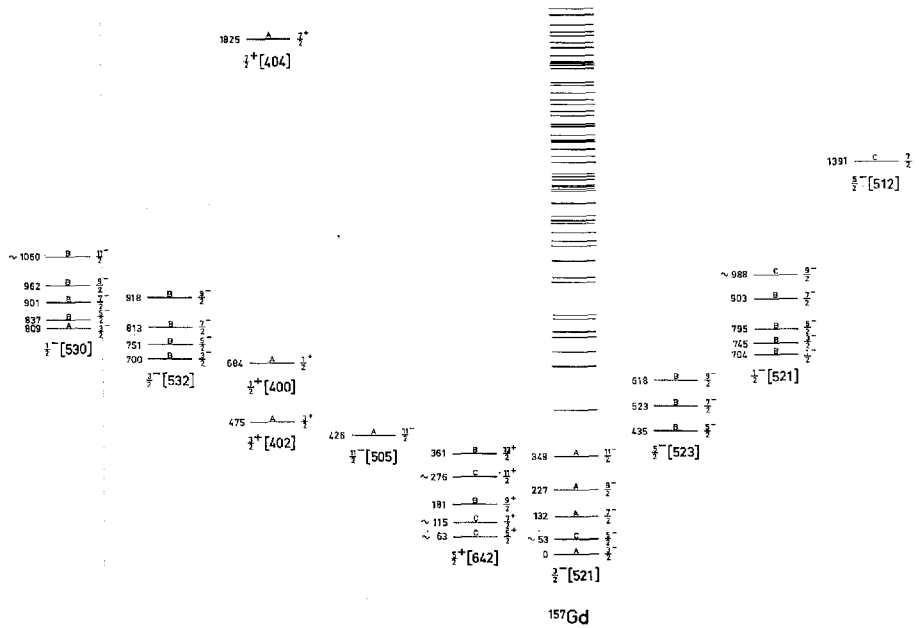

Fig. 19. Level scheme for ^{157}Gd.

certain. However, the absolute intensity of this state is somewhat larger than expected from the Nilsson wave functions.

4.3.9. The 5/2–[523] Orbital

This and the following sections discuss orbitals which are observed as particle excitations in the gadolinium nuclei. Most of the information comes therefore from the (d,p) spectra.

The $5/2-[523]$ orbital forms the ground state in ^{161}Gd. In this nucleus, all the rotational states up to the $11/2-$ state are observed with relative intensities in agreement with theoretical predictions. In ^{159}Gd, the band is expected as a low lying particle excitation, but no pattern similar to that in ^{161}Gd is observed below 700 keV. However, if the band head is placed at 146 keV, the 226 keV, the 327 keV and possibly the 455 keV levels form an acceptable $K = 5/2$ band. The 7/2 member of this band has a cross section approximately five times larger than expected for the 7/2 $5/2-[523]$ state. This deviation can be explained qualitatively by Coriolis coupling to the $3/2-[521]$ band which has a large cross section for the $7/2-$ state. Application of the formulae of sect. 2 shows that about 50 % of the observed

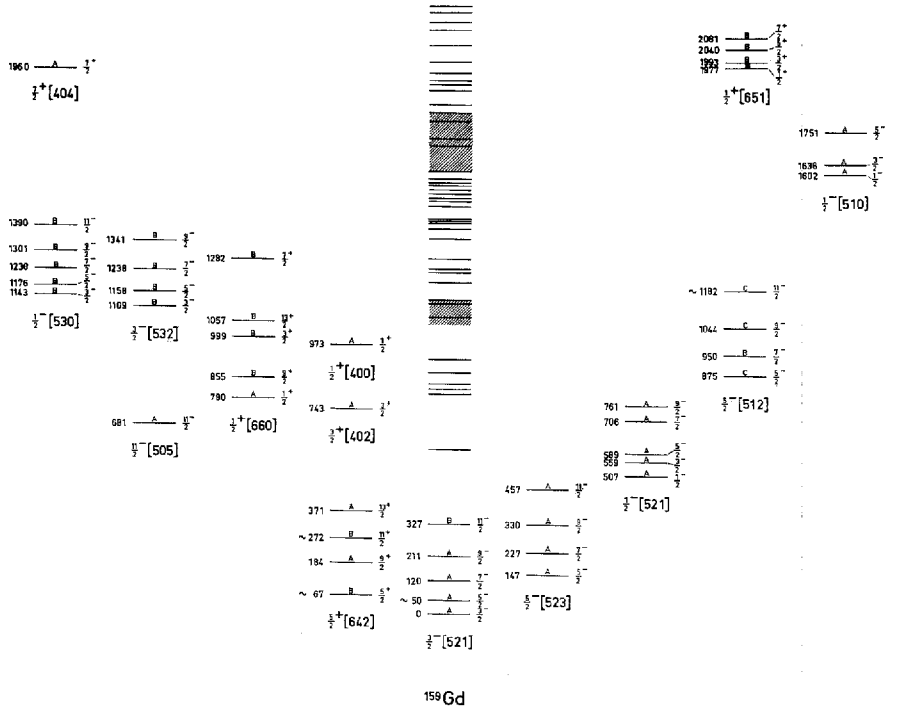

Fig. 20. Level scheme for ^{159}Gd.

cross section can be explained by the theoretical Coriolis matrix element between the two bands, which implies a 4 % admixture in the 7/2 state. It is furthermore worth mentioning that the calculated 7/2 − intensity is quite sensitive to changes in the deformation.

A band with a similar pattern is observed in ^{157}Gd with the band head at 435 keV. The cross section for the 7/2 − state is there approximately three times larger than expected for a pure state. The reduction in intensity compared to the ^{157}Gd case probably reflects the larger separation between the 5/2 − [523] and the 3/2 − [521] bands.

It has been proposed[20] that the 5/2 5/2 − [523] state in ^{155}Gd is found at 287 keV. In the (d,p) spectra, it is indeed possible to place the 5/2, 7/2, and 9/2 states of this band at 287 keV, 370 keV (hidden), and 485 keV, respectively, which yields an invertial parameter A = 12.4 keV. The intensity of the 5/2 − state is then significantly lower than expected. A somewhat different band is obtained if the above mentioned states are placed at 321 keV, 392 keV, and 485 keV, respectively, which yields A = 10.2 keV. These

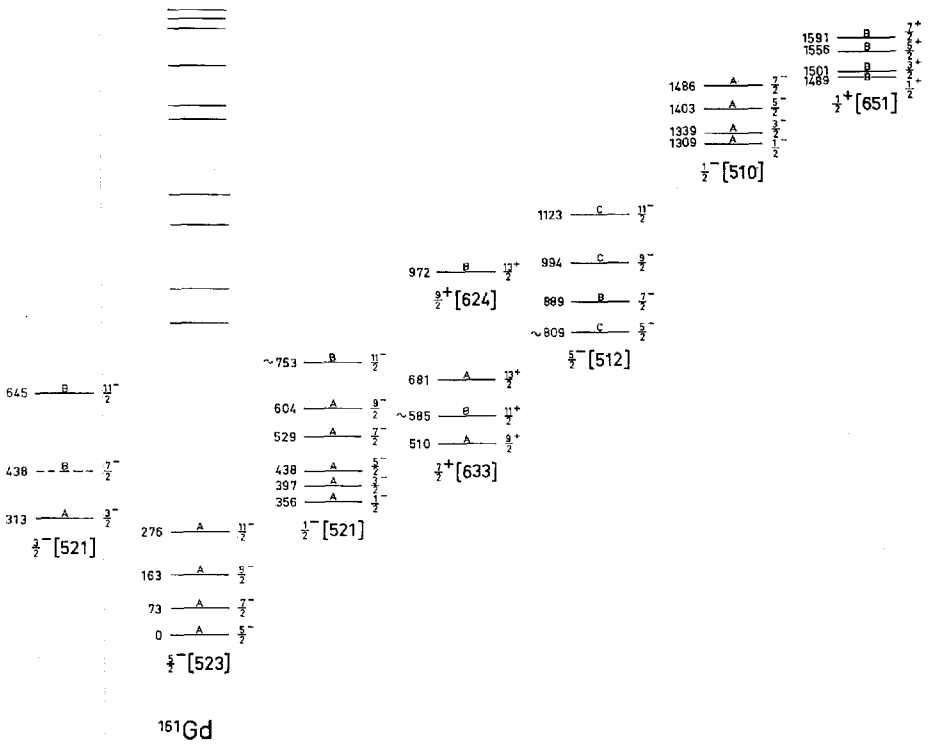

Fig. 21. Level scheme for ^{161}Gd.

states are populated in the (d, d') reaction[8] as expected from the Coriolis coupling to the ground state band. The latter band has therefore been preferred here and is shown in fig. 18.

4.3.10. The 1/2–[521] Orbital

This orbital should occur as a particle excitation in all the gadolinium nuclei. All the rotational states are expected to be populated with most of the intensity in the $1/2-$, $5/2-$, and $7/2-$ states. The theoretical decoupling parameter is 0.9 and the resulting pattern is highly characteristic of the orbital. The identification of the band is therefore quite certain in spite of significant differences between the observed and calculated absolute cross sections.

The cross sections for the rotational states in the $1/2-[521]$ show violent fluctuations, but the average values are in reasonable agreement with the theoretical predictions (fig. 24). Several effects can be responsible for this

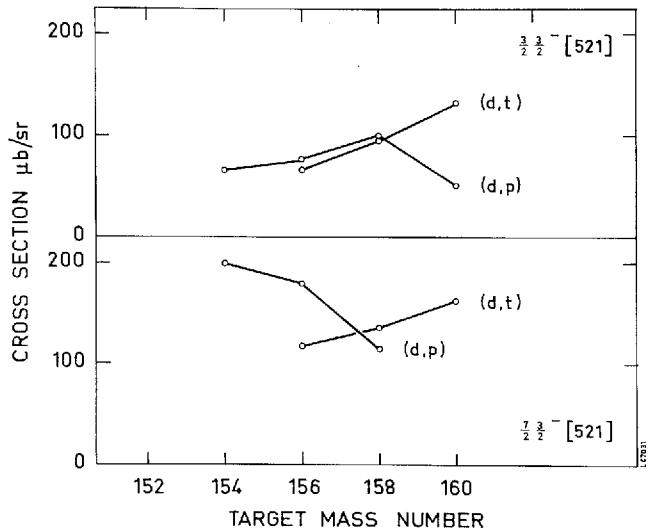

Fig. 22. Cross section for the 3/2 3/2 − [521] and 7/2 3/2 − [521] states as a function of the final mass number. The (d,p) cross sections are reduced to $Q = 3$ MeV and the (d,t) cross sections to $Q = -2$ MeV.

behaviour, the most important probably being the coupling to the gamma-vibrational states. Calculations by SOLOVIEV[23] show that, in ^{155}Gd, the lowest $1/2-$ state is 42 % $1/2-[521]$, 37 % gamma vibration based on the $3/2-[521]$ state, and 18 % gamma vibration based on the $5/2-[523]$ state. The (d,p) cross section obtained here seems to indicate a somewhat larger single-particle amplitude than given by SOLOVIEV; on the other hand, the predicted contribution from the gamma vibration based on the ground state is in very good agreement with the results obtained for ^{155}Gd in the (d,d') experiment[8]. The low cross section for the $1/2-[521]$ band in ^{157}Gd is somewhat surprising in view of the fact that this band is weakly populated in the (d,d') reaction. The decoupling parameters for the $1/2-[521]$ bands in the gadolinium isotopes are considerably smaller than the theoretical value, which is in agreement with observations for other bands with vibrational admixtures[19].

In addition to the coupling to the gamma vibration, the Coriolis coupling to the various $K = 1/2-$ and $3/2-$ bands can be expected to be of importance.

4.3.11. The 7/2 + [633] Orbital

The $7/2+[633]$ orbital is expected to be weakly populated and only in ^{161}Gd it has been possible to identify the band with some degree of certainty.

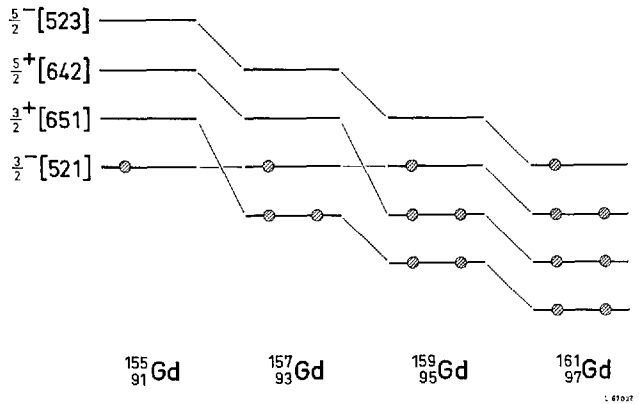

Fig. 23. Expected order of filling of Nilsson states in deformed Gd isotopes.

The groups corresponding to the 9/2 and 13/2 states shown in fig. 21 have reasonable intensities, and high l values are indicated by the angular intensity variations. The inertial parameter is $A = 6.4$ keV, in agreement with the generally high moment of inertia for this orbital.

4.3.12. The 5/2–[512] Orbital

This orbital is characterized by a strong $l = 3$ group to the $7/2-$ state. The ^{161}Gd spectrum has a strong proton group at 889 keV which appears to have $l = 3$; unfortunately, the group at 90° coincided with a plate joint. Nevertheless, this group has been assigned to the $7/2\ 5/2-[512]$ state, and a reasonable rotational band has been constructed (fig. 21). In ^{159}Gd, there is no single group with the expected intensity, but three groups at 950 keV, 1138 keV, and 1430 keV seem to have $l = 3$ and a combined reduced intensity corresponding to approximately 80 % of the intensity of the $7/2-$ group in ^{161}Gd. It is therefore indicated that, in ^{159}Gd, the strength in the $5/2-[512]$ orbital is shared between several levels. In ^{157}Gd, there is a single group at 1391 keV with $l = 3$, but the intensity is there only about 30 % of that in ^{161}Gd. It has not been possible to trace the $5/2-[512]$ orbital in the lighter gadolinium nuclei.

It is interesting to note the breakdown of the single-particle description for the $5/2-[512]$ orbital and also for the $1/2-[521]$ orbital in the gadolinium nuclei. In the ytterbium nuclei, these states occur near the ground state and show excellent agreement[1)] with the predictions based on pure Nilsson wave functions.

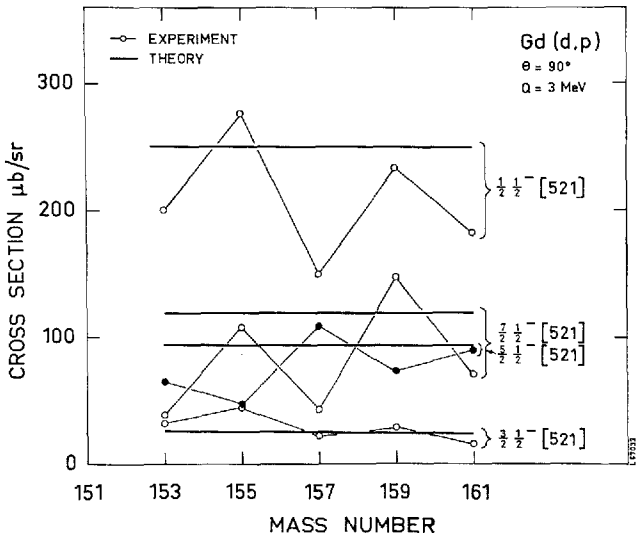

Fig. 24. Cross section for the (d,p) reaction of the $1/2-[521]$ state as a function of the final mass number. The cross section is reduced to $Q = 3$ MeV.

4.3.13. The 1/2–[510] Orbital

For this orbital, a strong $l = 1$ group is expected to the $3/2-$ level and relatively strong $l = 3$ groups to the $5/2-$ and $7/2-$ levels. The theoretical decoupling parameter is $a = -0.34$, but the experimentally determined decoupling parameters for this band in other nuclei are slightly positive.

In ^{161}Gd, the strong group at 1339 keV which has an $l = 1$ distribution is assigned to the $3/2-$ level of the $1/2-[510]$ band. The rotational band shown in fig. 21 is constructed from groups with nearly correct relative intensities (cf. table 19) and yields $a = -0.12$ and $A = 11.3$ keV. The total absolute cross section of the band is about 60 % of that expected for a pure state.

The ^{159}Gd spectrum has an intense peak at 1602 keV with an $l = 1$ angular dependence. If this peak is assigned to the $3/2-$ level, the rotational band shown in fig. 20 can be constructed from groups with reasonable intensities and angular distributions; however, the solution is not unique, since other groups are present in the same energy region. The band shown in fig. 20 corresponds to $a = 0.38$ and $A = 11.6$ keV. The total intensity is approximately 50 % of the calculated intensity.

In the (d,p) spectra of lighter nuclei, there are no single groups with as large intensities as those discussed above and it has therefore not been possible to identify the $1/2-[510]$ band or fractions thereof.

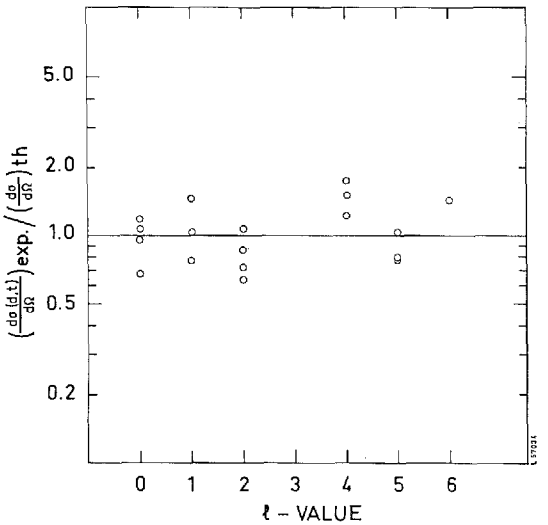

Fig. 25. Ratio of experimental to theoretical cross sections for states populated by (d,t) reactions.

4.3.14. The 1/2 + [651] Orbital

On the basis of the Nilsson diagram this orbital can be expected as a fairly low lying particle state in the well deformed nuclei. It is characterized by large cross sections (cf. table 10) to the 1/2, 3/2, 5/2, and 7/2 states and a decoupling parameter of -0.6 and should therefore be fairly easy to identify in the spectra. The band is not expected to be much affected by mixing, because the quantum numbers are different from those of the neighbouring levels.

The 1/2 + [651] orbital has been tentatively identified in ^{161}Gd and ^{159}Gd. In both nuclei, the four levels which are expected to be strongly populated have been observed with large cross sections, although the agreement with the predicted values is not perfect (cf. table 20). The parameters of the band in ^{161}Gd are $a = -0.47$ and $A = 7.6$ keV and, in ^{159}Gd, $a = -0.27$ and $A = 7.7$ keV.

The 1/2 + [651] band is expected at approximately 2.5 MeV in ^{157}Gd, but at this excitation energy the spectra are complicated and have not been analyzed.

4.3.15. Other Levels in the Deformed Nuclei

The level schemes, figs. 18–21, show a considerable number of levels for which it has not been possible to give a definite assignment to a single-particle orbital. Most of these levels are found at high excitation energies,

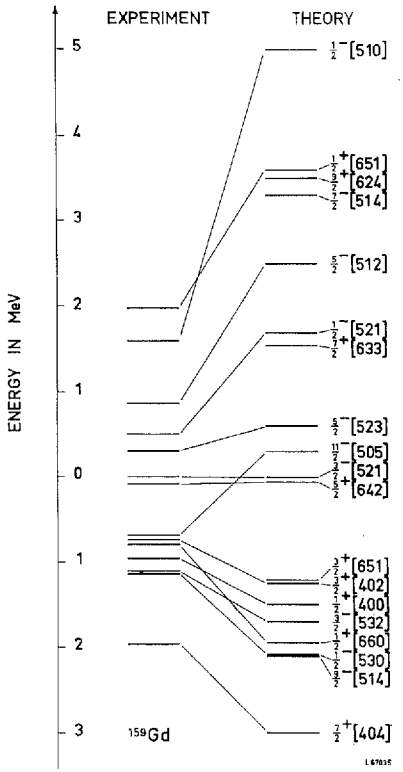

Fig. 26. Experimental and theoretical Nilsson levels in ^{159}Gd.

but especially the ^{155}Gd and the ^{157}Gd spectra show several low lying levels in this category, which are strongly populated by the transfer reactions. The discussion in the preceding sections has repeatedly touched upon the various types of couplings which can spread the single-particle intensity of several levels, and we shall here just mention a few unassigned levels for which it seems reasonable to make more definite statements.

The level at 972 keV in ^{161}Gd appears to have a high l-value, perhaps $l = 6$. In this region of the spectrum, the $9/2+[624]$ orbital is expected, and it is possible that the 972 keV level is the $13/2+$ level of this band. If this is the case, the $7/2-[514]$ orbital is the only particle excitation below the $1/2+[651]$ orbital which has not been identified in ^{161}Gd.

It has recently been suggested[20] that a beta-vibrational band with energies 592.6 keV $(3/2-)$ and 647.8 keV $(5/2-)$ occurs in ^{155}Gd. This suggestion is mostly based on the observation of an E0 component in the decay of these states. The present (d,t) data lend some support to the band pro-

posed. The groups at 594 keV, 721 keV, and 813 keV which could correspond to the 3/2−, 7/2−, and 9/2− members show intensity ratios of 1.00:1.89:0.37. These can be compared to the corresponding ratios 1.00: 1.92:0.22 for the ground-state band. The total (d,t) intensity to the excited band is approximately 25 % of that to the ground-state band. It should be remarked that the 7/2− state suggested here is different from the 706 keV state proposed in ref.[20]. The moment of inertia parameter A for the beta band is 10.6 keV compared to 12.1 keV for the ground-state band. The reduction in A is in agreement with the data for the beta vibrations in the even nuclei. The beta-vibrational band in ^{155}Gd is also observed in the (d,d') spectra[8].

4.3.16. Levels in ^{153}Gd and ^{151}Gd

On the basis of the present data, very little can be said about the nature of the levels in ^{153}Gd and ^{151}Gd.

It has been proposed[24] that the 3/2+[651] orbital forms the ground state in ^{153}Gd. This assignment is difficult to reconcile with the strong population observed here for the ground state and the 93 keV state. If indeed the ground-state spin[25] of ^{153}Gd is 3/2, then the present data rather point to a connection to the 3/2−[521] state. The properties of the level at 93 keV in ^{153}Gd resemble those of the mysterious level at 105 keV in ^{155}Gd (cf. sect. 4.3.2). The levels at 140 keV, 213 keV, 328 keV, 363 keV, and 1287 keV seem to be related to the 11/2−[505], 3/2+[402], 1/2+[400], 1/2−[530], and 7/2+[404] orbitals, respectively, and are discussed in the previous sections. Similarly, the 856 keV level has been assigned as the band head of a band related to the 1/2−[521] orbital.

In ^{151}Gd, even the ground-state spin is unknown. The ground state in the isotone ^{149}Sm has been assigned to the $f7/2$ shell-model state and the (d,t) data are consistent with the same assignment for the ^{151}Gd ground state. The levels at 977 keV and 1047 keV have been associated with the $d3/2$ and $s1/2$ shell-model states and are discussed in sect. 4.3.5.

5. Comparison of Intensities with Predicted Values

It is of considerable interest to compare the observed absolute intensities with those predicted from theory as outlined in sect. 2. A comparison of this kind was performed for the ytterbium isotopes which, on the average, showed good agreement between the (d,p) cross sections, whereas the calculated (d,t) cross sections were somewhat lower than the experimental

TABLE 12. (d,t) population of the $3/2-[521]$ band.

Spin	$d\sigma/d\Omega$, $\theta = 90°$, $Q = -2$ MeV				Relative values of C_{jl}^2			
	Theory	^{155}Gd	^{157}Gd	^{159}Gd	Theory	^{155}Gd	^{157}Gd	^{159}Gd
3/2	176	68	84	132	0.10	0.11	0.10	0.14
5/2	~ 0	~ 1	2	4	~ 0	~ 0.005	0.006	0.01
7/2	315	117	135	164	0.53	0.54	0.46	0.50
9/2	24	12	12	17	0.26	0.35	0.26	0.32
11/2	11	–	8	2	0.11	–	0.17	0.04

TABLE 13. (d,t) population of the $11/2-[505]$ band.
$d\sigma/d\Omega$, $\theta = 90°$, $Q = -2$ MeV.

Spin	Theory	^{158}Gd	^{155}Gd	^{157}Gd	^{159}Gd
11/2 –	94	48	119	74	96

TABLE 14. (d,t) population of the $N = 4$ states.
$d\sigma/d\Omega$, $\theta = 90°$, $Q = -2$ MeV.

Level	Theory	^{158}Gd	^{155}Gd	^{157}Gd	^{159}Gd
3/2 3/2 + [402]	678	717	488	435	586
1/2 1/2 + [400]	858	820	922	1015	642
7/2 7/2 + [404]	157	~ 270*	277	194	235

* Estimated from the yield at 60°.

TABLE 15. (d,t) population of the $1/2-[530]$ band.

Spin	$d\sigma/d\Omega$, $\theta = 90°$, $Q = -2$ MeV				Relative values of C_{jl}^2			
	Theory	^{155}Gd	^{157}Gd	^{159}Gd	Theory	^{155}Gd	^{157}Gd	^{159}Gd
1/2	10	27	–	–	0.006	0.02	–	–
3/2	357	554	365	275	0.21	0.35	0.40	0.29
5/2	35	165	58	10	0.06	0.30	0.18	0.03
7/2	137	100	29	48	0.23	0.18	0.07	0.14
9/2	30	13	18	18	0.35	0.15	0.35	0.31
11/2	14	–	–	13	0.15	–	–	0.24

TABLE 16. (d,p) population of the $3/2-[521]$ band.

Spin	$d\sigma/d\Omega$, $\theta = 90°$, $Q = 3$ MeV					Relative values of C_{jl}^2				
	Theory	^{155}Gd	^{157}Gd	^{159}Gd	^{161}Gd	Theory	^{155}Gd	^{157}Gd	^{159}Gd	^{161}Gd
3/2	107	64	76	91	53	0.10	0.10	0.12	0.30	0.11
5/2	0	–	–	–	–	0	–	–	–	–
7/2	275	192	177	105	120	0.53	0.59	0.57	0.70	0.47
9/2	17	13	12	–	–	0.26	0.32	0.32	–	–
11/2	8	–	–	–	14	0.11	–	–	–	0.42

TABLE 17. (d,p) population of the $5/2-[523]$ band.

Spin	$d\sigma/d\Omega$, $\theta = 90°$, $Q = 3$ MeV					Relative values of C_{jl}^2				
	Theory	^{155}Gd	^{157}Gd	^{159}Gd	^{161}Gd	Theory	^{155}Gd	^{157}Gd	^{159}Gd	^{161}Gd
5/2	39	37	34	48	22	0.07	0.11	0.11	0.10	0.08
7/2	40	113	124	112	~21	0.08	0.33	0.39	0.28	0.08
9/2	54	25	20	~14	22	0.79	0.56	0.50	0.27	0.64
11/2	4	–	–	18	7	0.06	–	–	0.35	0.20

TABLE 18. (d,p) population of the $1/2-[521]$ band.

Spin	$d\sigma/d\Omega$, $\theta = 90°$, $Q = 3$ MeV						Relative values of C_{jl}^2					
	Theory	^{153}Gd	^{155}Gd	^{157}Gd	^{159}Gd	^{161}Gd	Theory	^{153}Gd	^{155}Gd	^{157}Gd	^{159}Gd	^{161}Gd
1/2	255	200	252	151	213	171	0.25	0.39	0.35	0.32	0.23	0.25
3/2	25	31	43	22	27	15	0.02	0.06	0.06	0.05	0.03	0.02
5/2	95	63	43	110	68	~85	0.18	0.24	0.12	0.46	0.15	0.24
7/2	120	38	110	43	135	86	0.23	0.15	0.25	0.18	0.29	0.19
9/2	18	6	11	–	18	13	0.27	0.17	0.23	–	0.30	0.29
11/2	3	–	–	–	–	–	0.05	–	–	–	–	–

TABLE 19. (d,p) population of the $1/2-[510]$ band.

Spin	$d\sigma/d\Omega$, $\theta = 90°$, $Q = 3$ MeV			Relative values of C_{jl}^2		
	Theory	^{159}Gd	^{161}Gd	Theory	^{159}Gd	^{161}Gd
1/2	10	–	4	0.01	–	0.01
3/2	414	198	210	0.41	0.50	0.50
5/2	151	67	70	0.29	0.34	0.33
7/2	100	31	33	0.19	0.16	0.15
9/2	6	–	–	0.09	–	–
11/2	1	–	–	0.02	–	–

TABLE 20. (d,p) population of the $1/2+[651]$ band.

Spin	$d\sigma/d\Omega$, $\theta = 90°$, $Q = 3$ MeV			Relative values of C_{jl}^2		
	Theory	^{159}Gd	^{161}Gd	Theory	^{159}Gd	^{161}Gd
1/2	120	82	111	0.070	0.16	0.17
3/2	137	70	81	0.13	0.22	0.20
5/2	171	88	191	0.17	0.28	0.40
7/2	65	29	26	0.23	0.34	0.23
9/2	16	–	–	0.06	–	–
11/2	10	–	–	0.22	–	–
13/2	6	–	–	0.13	–	–

values. As the cross-section systematics strongly indicated that the states in Yb did correspond to almost pure single-particle excitations, it was concluded that the DWBA results for the (d,p) reaction were quite accurate, whereas the particular DWBA calculation used for the (d,t) reaction was not entirely satisfactory.

For the gadolinium isotopes considered here, a comparison of experimental and theoretical (d,p) cross sections is not very meaningful as a check on the DWBA results. The discussion in sect. 4 shows that almost none of the states observed as particle excitations corresponds to pure configurations. However, the optical model parameters used in the calculations are identical to those used for ytterbium, and there is good reason to believe that they should work well for gadolinium too. The ratios of observed to calculated (d,p) cross sections can then be taken as measures of the purities of the particle states observed.

Tables 16 to 20 compare the reduced (d,p) cross sections to those obtained from the theoretical wave functions and the DWBA results with the parameters listed in table 1. It is evident that, in most cases, the observed cross sections are lower than predicted, in agreement with the discussion in sect. 4. Apart from the cases where strong Coriolis couplings significantly affect the cross sections, the relative intensities to the rotational states within a band are in reasonable agreement with the theory.

The situation with respect to the (d,t) cross sections is somewhat different because of the poor agreement between the experimental and theoretical cross sections for the ytterbium isotopes. The parameters used for gadolinium (table 1) are probably superior to the earlier ytterbium parameters, but again, in the gadolinium isotopes there is a lack of states which can be assumed to be pure single-hole excitations. Nevertheless, a comparison of

the cross sections for selected cases shows reasonable agreement between experimental and theoretical values. These cases are listed in tables 12 to 15. Fig. 25, which corresponds to fig. 24 of ref.[1]), shows that the agreement between experiment and theory for the low l values is considerably better than for ytterbium. However, the cross sections for the high l-values appear to be somewhat too high, in agreement with the observations for ytterbium.

As a further check on the accuracy of the DWBA results, the (d,t) parameters listed in table 1 were used for the ytterbium nuclei. The ratios of experimental to theoretical cross sections thus obtained were considerably closer to unity than the earlier results, but the procedures are still too uncertain to allow a precise determination of spectroscopic factors from the (d,t) reaction.

6. Conclusions

The present survey of the single-neutron transfer reactions to the odd gadolinium isotopes identifies rotational bands which correspond to 16 different Nilsson orbitals. Most of these bands or parts thereof have been observed in several final nuclei.

In many cases, it is indicated that the rotational bands based on the single-particle excitations are considerably mixed with each other and with bands based on collective states. In all the nuclei, several levels are observed for which no assignment can be made.

The single-particle levels observed span a considerable range of energies. Fig. 26 shows the theoretical Nilsson levels for a deformation of $\beta = 0.3$ and $\hbar\omega = 8.8$ MeV together with the experimentally observed levels in ^{159}Gd. The observed level order in general agrees with the theoretical one, except for the $11/2-[505]$ level which occurs considerably lower than expected. The experimental energy scale is compressed almost a factor of two compared to the theoretical scale. This effect has been observed earlier and can, at least in part, be ascribed to the pairing interaction which can be estimated to reduce the energy span by $\sim 2\Delta$ or approximately 2.5 MeV. If one considers that the $1/2-[510]$ level is lowered by the gamma vibration, this expectation is in reasonable agreement with the observations.

It should be remarked that fig. 26 includes levels from the $N = 4$, 5, and 6 oscillator shells. Especially important is the simultaneous observation of the $7/2+[404]$ and the $1/2+[651]$ orbitals, which fixes the relative positions of the $1g\,7/2$ and $2g\,9/2$ shell-model states. The observation of components of these distant single-particle levels in one nucleus reflects the tremendous change in the single-particle levels caused by the deformation.

Acknowledgements

The authors want to thank R. BLOCH for assistance in some of the measurements and ANNA GRETE JØRGENSEN and GUNVER DAMM JENSEN for careful plate scanning. This work has greatly profited from the excellent targets prepared by G. SØRENSEN, J. THORSAGER, and V. TOFT at the University of Aarhus Isotope Separator. Finally, P. O. TJØM acknowledges support from Norges Teknisk-Naturvitenskapelige Forskningsråd.

The Niels Bohr Institute
University of Copenhagen

References

1) D. G. Burke, B. Zeidman, B. Elbek, B. Herskind and M. C. Olesen, Mat. Fys. Medd. Dan. Vid. Selsk. **35**, nr. 2 (1966).
2) S. G. Nilsson, Mat. Fys. Medd. Dan. Vid. Selsk, **29**, nr. 16 (1955).
3) R. H. Bassel, R. M. Drisko and G. R. Satchler, ORNL Report **3240** (unpublished).
4) D. R. Bès and Cho Yi-chung, Nuclear Physics **86** (1966) 581.
5) R. Bloch, B. Elbek and P. O. Tjøm, Nuclear Physics A **91** (1967) 576.
6) D. G. Burke and B. Elbek, Mat. Fys. Medd. Dan. Vid. Selsk. to be published.
7) M. Jaskola, K. Nybø, P. O. Tjøm and B. Elbek, Nuclear Physics A **96** (1967) 52.
8) F. Sterba, P. O. Tjøm and B. Elbek, to be published.
9) G. R. Satchler, Ann. Phys. **3** (1958) 275.
10) M. N. Vergnes and R. K. Sheline, Phys. Rev. **132** (1963) 1736.
11) C. W. Reich and M. E. Bunker, unpublished.
12) B. E. Chi, Nuclear Physics **83** (1966) 97.
13) R. K. Cooper and J. Bang, The Niels Bohr Institute, G.A.P. **2** (1965).
14) A. K. Kerman, Mat. Fys. Medd. Dan. Vid. Selsk. **30**, no. 15 (1956).
15) A. Bohr and B. R. Mottelson, Lecture Notes (Copenhagen 1966).
16) P. O. Tjøm and B. Elbek, to be published.
17) S. Whineray, private communication (1967).
18) S. G. Nilsson, private communication (1966).
19) R. M. Diamond, B. Elbek and F. S. Stephens, Nuclear Physics **43** (1963) 560.
20) M. Finger, P. Galan, J. Urbanzc (Dubna), private communication (1966).
21) M. Jaskola, B. Elbek and P. O. Tjøm, to be published.
22) J. Borggreen, L. Westgaard and N. J. S. Hansen, Nuclear Physics A **95** (1967) 202.
23) V. G. Soloviev, private communication (1966).
24) B. Harmatz, T. H. Handley and J. W. Mihelich, Phys. Rev. **128** (1962) 1186.
25) D. Ali, Nuclear Physics **71** (1965) 441.
26) I. J. Spalding and K. F. Smith, Proc. Phys. Soc. (London) **79** (1962) 787.

Indleveret til Selskabet den 1. juli 1967.
Færdig fra trykkeriet den 31. december 1967.